ROLE OF INERT GAS TO REDUCE MECHANICAL DEFECTS OF THE BUILT OBJECT FABRICATED BY SLM PROCESS

MOHAMED I HAMED ELGADARI

FACULTY OF ENGINEERING/MECHANICAL ENGINEERING DEPARTMENT
UNIVERSITY OF MALAYA
KUALA LUMPUR

2018

ROLE OF INERT GAS TO REDUCE MECHANICAL DEFECTS OF THE BUILT OBJECT FABRICATED BY SLM PROCESS

MOHAMED I HAMED ELGADARI

THESIS SUBMITTED IN FULFILMENT OF THE REQUIREMENTS FOR THE DEGREE OF MASTER IN MECHANICAL ENGINEERING

FACULTY OF ENGINEERING
UNIVERSITY OF MALAYA
KUALA LUMPUR

2018

UNIVERSITY OF MALAYA

ORIGINAL LITERARY WORK DECLARATION

Name of Candidate: Mohamed I Hamed Elgadari (I.C/Passport No:)

Matric No: KQK 160014

Name of Degree: Master of Mechanical Engineering

Title of Research Report ("ROLE OF INERT GAS TO REDUCE MECHANICAL DEFECTS OF THE BUILT OBJECT"):

Field of Study: Material Science

I do solemnly and sincerely declare that:

(1) I am the sole author/writer of this Work;
(2) This Work is original;
(3) Any use of any work in which copyright exists was done by way of fair dealing and for permitted purposes and any excerpt or extract from, or reference to or reproduction of any copyright work has been disclosed expressly and sufficiently and the title of the Work and its authorship have been acknowledged in this Work;
(4) I do not have any actual knowledge nor do I ought reasonably to know that the making of this work constitutes an infringement of any copyright work;
(5) I hereby assign all and every rights in the copyright to this Work to the University of Malaya ("UM"), who henceforth shall be owner of the copyright in this Work and that any reproduction or use in any form or by any means whatsoever is prohibited without the written consent of UM having been first had and obtained;
(6) I am fully aware that if in the course of making this Work I have infringed any copyright whether intentionally or otherwise, I may be subject to legal action or any other action as may be determined by UM.

Candidate's Signature Date:

Subscribed and solemnly declared before,

Witness's Signature Date:

Name:

Designation:

ROLE OF INERT GAS TO REDUCE MECHANICAL DEFECTS OF THE BUILT OBJECT FABRICATED BY SLM PROCESS

ABSTRACT

The use of additive manufacturing (AM) technology has been expanding dramatically last few decades, especially in the industrial sector. The need of switching from the mass production to individual production has led to increase the interest to the additive manufacturing especially selective laser melting (SLM). The quality of a SLM object depends on few parameters such as laser power, scanning speed, and inert gas. In this project, the effect of inert gas on the microstructure and mechanical properties of an austenitic stainless steel was investigated. For this reason, two samples were studied. At the beginning of the manufacturing process, the Argon gas was present. However, near to the end of the process, the Argon gas had run out and the process continued without an inert gas. The laser power used for both samples was 360 W while scanning speeds were 250 and 510 mm/s respectively. The tensile strength as well as micro hardness was studied to investigate the mechanical properties. Microstructure observation was performed using optical microscope and (SEM). Microstructure for both samples was performed in 3 sections which represent the lower, middle and upper part of the sample. Results show that, high porosity was observed in section 3 while in the other sections the porosity status was lower than section 3. Microhardness test showed that, the average hardness at section 3 for sample 1 and 2 was 192 and 205 HV which is higher than other sections. Tensile test results show that the ultimate tensile strength and yield strength for sample 1 were 482 MPa and 245 MPa respectively. However tensile results for sample 2 showed an enhancement on these properties. After the samples were broken, it was noted that the fraction occurred at a section near to the top of the sample which was formed after finishing the inert gas. The reason for that might be due to the high porosity at that section that caused stress concentration.

PERANAN GAS LENGAI UNTUK MENGURANGKAN KECACATAN MEKANIKAL OBJEK TERBINA YANG DIBUAT OLEH PROSES SLM

ABSTRAK

Penggunaan teknologi pengilangan bahan tambahan (AM) telah berkembang secara dramatik beberapa dekad yang lalu, terutamanya dalam sektor perindustrian. Keperluan beralih dari pengeluaran besar-besaran ke pengeluaran individu telah membawa kepada peningkatan minat terhadap pembuatan tambahan terutamanya pencairan laser terpilih (SLM). Kualiti objek SLM bergantung kepada beberapa parameter seperti kuasa laser, kelajuan pengimbasan, dan gas lengai. Dalam projek ini, kesan gas lengai pada struktur mikro dan sifat mekanik keluli tahan karat austenit telah disiasat. Atas sebab ini, dua sampel telah dipelajari. Pada permulaan proses pembuatan, gas Argon hadir. Bagaimanapun, hampir ke penghujung proses, gas Argon telah habis dan prosesnya terus tanpa gas lengai. Kuasa laser yang digunakan untuk kedua-dua sampel ialah 360 W manakala kelajuan pengimbasan masing-masing adalah 250 dan 510 mm / s. Kekuatan tegangan serta kekerasan mikro dikaji untuk menyiasat sifat-sifat mekanik. Pemerhatian mikro dilakukan menggunakan mikroskop optik dan (SEM). Struktur mikro untuk kedua-dua sampel dilakukan dalam 3 bahagian yang mewakili bahagian bawah, bahagian tengah dan atas sampel. Keputusan menunjukkan bahawa keliangan yang tinggi telah diperhatikan dalam bahagian 3 manakala dalam bahagian lain, status keliangan lebih rendah daripada bahagian 3. Ujian kemanjuran menunjukkan bahawa kekerasan purata pada bahagian 3 untuk sampel 1 dan 2 ialah 192 dan 205 HV yang lebih tinggi daripada bahagian lain. Keputusan ujian tegangan menunjukkan bahawa kekuatan tegangan muktamad dan kekuatan hasil untuk sampel 1 masing-masing adalah 482 MPa dan 245 MPa. Walau bagaimanapun keputusan tegangan untuk sampel 2 menunjukkan peningkatan pada sifat-sifat ini. Selepas sampel pecah, diperhatikan bahawa pecahan berlaku di bahagian berhampiran dengan bahagian atas sampel yang terbentuk selepas

menamatkan gas lengai. Sebabnya mungkin disebabkan porositi yang tinggi di bahagian itu yang menyebabkan kepekatan tekanan.

ACKNOWLEDGEMENTS

First and foremost, I would like to thank Allah, the Almighty, for affording me the opportunity to study for this degree and allowing me to experience many joys of life. Special thanks and appreciation go to my supervisor, Dr. Tuan Zaharinie, for first introducing me to the field of additive manufacturing and to her constructive suggestions, inspiration, and support, and for giving me great freedom in pursuing independent research. I wish to dedicate this work to my parents, my spouse, and my kids. This work would not have been completed without their endless patience and understanding, unwavering support and prayers, encouragement, and love. With this experience, I feel that I have performed great achievements and experienced great happiness during this course. I would also like to take this opportunity to express my thanks and gratitude to the many people who have helped me along my journey at University of Malaya, without whom my project would not have been completed successfully. I also would like to thank Mr. Kamarulazwan, Mr. Amirul and Ms. Aqilah for their advice and unlimited encouragement. I would also like to thank all technicians in the laboratories of the mechanical engineering department for their help and support. Finally, I am sure that I have missed to mention all of those who have contributed to the success of this project, but be sure that I love you all.

TABLE OF CONTENTS

LIST OF FIGURES

LIST OF TABLES

LIST OF SYMBOLS AND ABBREVIATIONS

SLM	:	Selective laser melting
AM	:	Additive manufacturing
SLS	:	Selective laser sintering
DMLS	:	Direct metal laser sintering
CNC	:	Computer numerical control
SM	:	Subtractive manufacturing

CHAPTER 1: INTRODUCTION

1.1 Motivation and background

The demand for rapid and cheaper fabricating processes has increased a lot during the last decades. The fabrication of parts that have high performance by the use of traditional techniques such like machining and casting are not efficient and it consumes a lot of time. The continues improvement on the manufacturing technology gave the opportunity for rapid prototyping technology to be improved. Due to the capability for the rapid prototyping that is not limited to a special designed tooling and featuring, nearly any complex design can be fabricated at high accuracy (Yasa & Kruth, 2011). According to the definition provided the ASTM additive manufacturing (AM) is the process of joining materials layer by layer to make a product by using computer aid design (CAD) (Baumann & Roller, 2017).

The concept in additive manufacturing is different than Subtractive Manufacturing (SM). In subtractive manufacturing the piece is produced by removing the material from the stock until it meets the required geometry while in additive manufacturing, the product is fabricated by adding the material layer by layer to get the final shape of the product. Each layer of the material is held to the preceding layer by the use of the heat produced by the laser beam. Earlier, the additive manufacturing technology was employed to fabricate prototypes or any small quantity of products. Nowadays, the additive manufacturing (AM) is not only used in fabricating prototypes but also it is used in number of applications such like modeling, fabricating tools and the end-use parts fabrication in small and medium sizes (Campbell & Ivanova, 2013). Additive manufacturing directly transfers the three-dimensional models that produced by computer aid design into physical parts. The additive manufacturing machine receives the data of the model in a series of thin sliced sections that represents the layers of the final product. Because of the absence of molds or tools, additive manufacturing has its advantage on

reducing not only the cost but also reduces the production time and its able to produce 3D complex products with high performance. Additive manufacturing also has the advantage to be a zero waste process since it is possible to use recycled feedstock materials. Consequently, the emissions will be reduced due to the reduction on the need of producing raw materials. Additionally, additive manufacturing process doesn't require the use of toxic chemicals contrary to other traditional manufacturing processes which needs lubricants and coolants (Herzog, Seyda, Wycisk, & Emmelmann, 2016).

The increasing demand on the quick productions of the items in order to put the products on the market as quick as possible has led to the invention of some additive manufacturing techniques. Nowadays, there are different additive manufacturing processes available on the market such as laser melt deposition (LMD), selective laser sintering (SLS) and selective laser melting (SLM). Each of these processes is distinguished by the type of the raw material used and by the criterial of consolidation such like conductive heating, laser melting and chemical reaction.

Many of additive manufacturing technologies uses energy beam in the consolidation process. These several processing mechanisms can be classified as bellow:

- Partial melting, which uses a mixture of two metallic powders. There are some common problems that could occur during this process such like insufficient densification, heterogeneous microstructure, and the variation in the properties. To solve these problems, further processing treatment is needed such as secondary infiltration with low melting point materials is often used.
- Indirect processing, where the powders of the metal are combined with polymer binders. This criterion exploits the presence of low melt point binder to consolidate the green part.

- Full melting, which is the most modern method, using fully melted metallic powders. The laser melting mechanism was developed to get fully dense parts and to reduce the time processing cycle. The concept of this mechanism is supported by continuous improvements in the conditions of laser processing, including laser types, higher laser powers, smaller focus spot sizes, and smaller layer thicknesses, which have in turn led to significant enhancements in the mechanical properties and microstructure of the fabricated objects, relative to those made with earlier lasers (Dadbakhsh, Hao, & Sewell, 2012). Among mentioned methods, Selective laser melting (SLM) uses metallic powder and laser beam in order to consolidate the part. This technology is able to produce objects with fully dense and do not need much of post processing.

The results yielded by the first two approaches are two-phased materials with low-melting-point constituents. These are mainly applied to rapid tooling. Whereas the fully melting method is more suitable to fabricate parts that do not need further treatment and can be used in different sectors (Faria, Godefroid, & Nery, 2016). The mechanical properties as well as dimensional tolerance and surface condition of the fabricated objects are mainly depending on the complex metallurgical and atom mechanism (Fera, Fruggiero, Lambiase, Macchiaroli, & Pham, 2016).

In SLM, the metallic powder is completely melted to the liquid phase and then rapidly cooled. The homogeneity of the product is easily controllable, but there are drawbacks. Because of the wide temperature variation during melting and cooling, residual stresses introduced into the product from thermal expansion and contraction may compromise the strength of the material. Additionally, defects such as porosity and balling may form during the phase transitions inherent to the build process.

1.2 Problem statement

This study investigates the effect of inert gas on the microstructure and the mechanical properties of 316L stainless steel fabricated by using selective laser melting technology (SLM). Commonly, the stainless steel grade 316L consists about 17% of the weight Cr and about 10% to 14% of the weight Ni. This kind of stainless steel is employed in the applications which requires material that has a high ductility as well as a good resistance such as furnace parts, heat exchangers, jet engine parts, pharmaceutical and photographic equipment.

The Additive manufacturing such as Selective Laser Melting (SLM) is a promising technique due its great potential and opportunity. The ability of fabricating complex structure with high mechanical properties grab the attention of studying this technology and examine its process parameters in order to get the best out of this technology. The laser power, scanning speed, building direction and other parameters are extensively studied and examined. Yet there are only few studies that examined the effect of inert gas on the microstructure and the mechanical properties of 316L stainless steel. This project will study this effect by using few samples that was fabricated initially with the present of Argon gas and at the end with the absence of the Argon gas.

1.3 Objectives

The objective of this study is to determine by using experimental measurements the effect of inert gas on

- The microstructure and porosity of the built object.
- The hardness of the built object.
- Mechanical properties such as ultimate tensile strength, yield strength and modulus of elasticity.

For this reason, the stainless steel samples were examined using available laboratory equipment to analyze the microstructure and the mechanical properties. Moreover, in this study the effect of the scanning speed also discussed.

CHAPTER 2: LITERATURE REVIEW

2.1 The history of laser additive manufacturing technology

Different techniques of additive manufacturing have been introduced since 19th century, where the topographical maps were created by using layering method. At that era, single layers were fabricated individually and then the they placed manually. Even though it was not a very precise technique, it achieved what is needed at that era. In the seventieth of the previous century, a new technique was introduced for maps fabrication. The technique involves exposing photo hardening material to a heat source. Later in 1970s, laser sintering process technology was proposed in a patent (Al-Meslemi, Anwer, & Mathieu, 2018).

The selective laser melting technique (SLM) is modern development from the selective laser sintering (SLS) which was invented earlier. The major difference between these two technologies is that: SLM melts metal powder of a specific thickness by using a high energy fiber laser whereas in SLS the powder is melted by using the classical CO_2 laser (Kruth, Levy, Klocke, & Childs, 2007). Figure (2.1) shows the microstructure of steel parts that were fabricated by using SLM and SLS respectively.

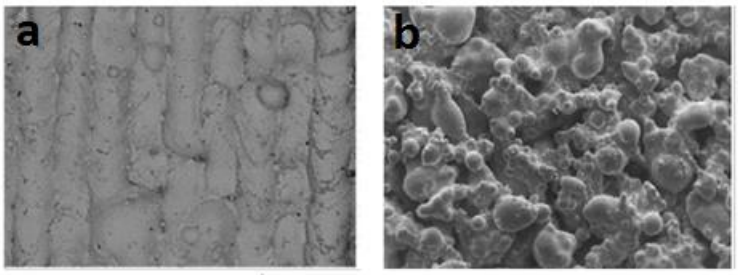

Figure 2.1: Surface structure of 316L stainless steel object produced by (a) SLS, (b) SLM (Kruth et al., 2007).

2.2 Powder generation for SLM

There are mainly two operations usually used in the creation of the powder for additive manufacturing applications. One of which is gas atomization and the other is water atomization. The both atomization processes have the similar theory to create the powder, however, the characteristics of the created powder is different, specifically for the particle shape aspect. The gas and water have different thermal capacities where the thermal capacity in the water is higher than thermal capacity in the gas. For this reason, by using gas atomization the alloy is cooled to a low temperature. By passing the metal liquid to the atomization medium the stream of the gas works to fog the liquid into small droplets. Since the gas has smaller thermal capacity, the droplet does not solidify immediately that grants the droplets some time to shrink and change to ball shapes as they fall. So a metal powder that has a spherical shape can be obtained by using gas atomization. On the other hand, since the water has higher thermal capacity, the droplets of the metal liquid solidify in a short time. So the droplets do not have the time to change the shape and they solidify immediately. For this reason, the powder created by the water atomization have irregular shapes. It is also possible to produce spherical shaped powder by using water atomization. This is can be done by controlling the atomization parameters such as super heating of

the metal liquid. There are no differences in the chemical composition of the powder due to the change in the production process regardless the atomization method used. Some alloys are sensitive to the oxygen. The content of the oxygen in any powder is basically relative to the oxygen sensitivity of the alloy itself. The oxygen content for most of the alloys can be minimized by minimizing the contact between the alloy and the oxygen during the atomization process. The gas atomization often employs the nitrogen gas as an atomization medium. The benefit of using the nitrogen gas is that; a huge count of nitrogen fills the atomization region that will evacuate the oxygen from the atomization region. So the nitrogen will preserve the droplets from oxidation through the atomization process (Raghunath & Pandey, 2007).

2.3 Selective Laser melting (SLM) development

Pierre Giraud, in 1971, documented a patent application illustrating criteria that is able to fabricate parts of complex geometry by placing metal powder on a substrate and using an energy beam such like laser to condense the powder. In 1980s, Dekard filed a patent application for SLS, that was commercialized by the evolution of DTM Sinter station 2000/2500 and powder materials feedstock. In 1995, the direct metal laser sintering (DMLS) machine was introduced to fabricate metallic parts for injection molding machines. The Selective Laser Melting (SLM) was invented in 1995 in Germany (Al-Meslemi et al., 2018).

2.3.1 Principles of SLM process and kinetic

Figure 2.2 shows the sequence of AM process. The first stage of fabricating an object by using AM including SLM is the designing of a CAD model for that object then converting it into STL file (stereolithography). The STL file is a three-dimensional representation of the object geometry. The geometry is divided into a set triangular facets. The larger the number of triangles, the better accuracy of the geometry surface. After that,

the STL file converted into 2D planes that represents the cross sectional layers with a specified thickness. The time required to build the object is determined by the orientation deposition path. Finally, the data then passed to the SLM machine in order to start manufacturing by directing and focusing the laser beam on metal powder layer. The substrate moves vertically to keep a constant space between the powder and the laser head. The laser continuously builds the object layer after layer by melting and fusing the layers together.

Figure 2.2: the sequence of AM processes starting from 3D model and finishing to manufactured part

A systematic drawing that illustrates the basic setup of SLM technology is shown in the figure (2.3). The building platform is supported by the building piston. The laser beam traces the sections and slices the surface constituting the geometry of the object. When the fabricating of the layer is done, the building piston step vertically down for a distance similar to the layer thickness. Then a new layer of the metal powder is placed on the building platform by the recoated arm. The process continuously progress until the whole object is formed. The majority of SLM processes is running with the present of inert gas in order to reduce the oxidation and porosity of the built object (Sames, List, Pannala, Dehoff, & Babu, 2016).

After the object is completely formed, the extra powder should be unloaded and the building platform is removed from the machine. Some extra post processing may be needed at this point in order to improve the surface condition as well as the mechanical properties.

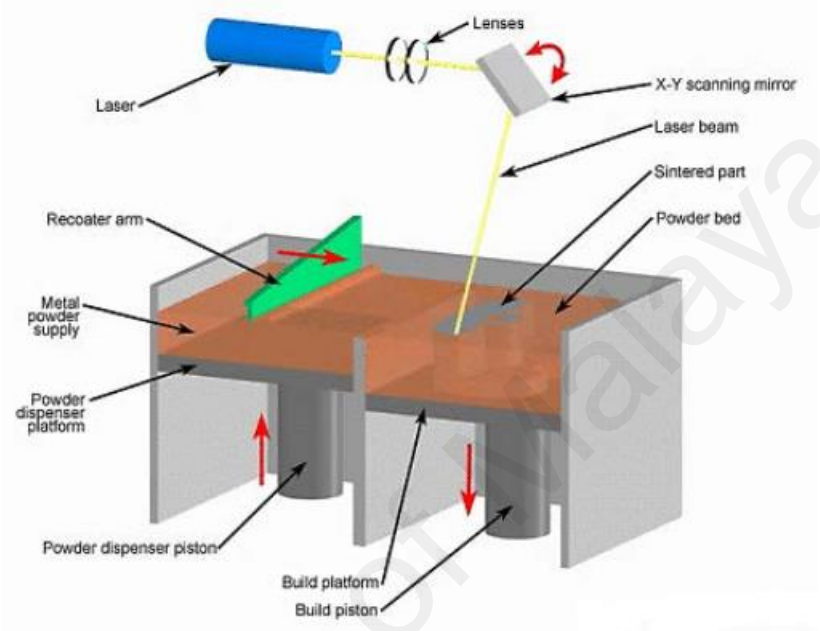

Figure 2.3: systematic drawing of SLM process (Sames et al., 2016).

The cooling–heating cycle of the building process must be considered when selecting SLM over other AM methods, because materials that are sensitive to constant thermal cycling may exhibit properties that are different to those which were originally intended under constant temperature fluctuations. The effects of thermal expansion and contraction occurring during the thermal cycles of the SLM build process often lead to the development of more residual stress in products than in those procured through traditional manufacturing processes; these stresses can lead to critical defects of cracking and delamination. Furthermore, if the build temperature is poorly controlled, the molten powder may ball up, which effectively ruins the build (DebRoy et al., 2018). If the powder feedstock is allowed to melt, the grain formation and orientation become inconsistent,

adversely affecting the quality of the build. Therefore, temperature control is necessary for the success of an SLM build (Rajabi, Vahidi, Simchi, & Davami, 2009).

2.4 Additive Manufacturing VS Traditional Manufacturing

One major difference between AM and traditional manufacturing, such as computer numeric control (CNC) machining, is that machining generally employs cutting oil for lubrication, which becomes waste that accompanies the removed material. The pollution of terrestrial, aquatic, and atmospheric systems resulting from AM methods is much lower than that resulting from traditional manufacturing processes; the main health risk associated with traditional manufacturing processes is the oil mist formed by the metalworking fluids. Therefore, it is necessary to measure toxicity and as many other factors as possible, rather than judging the level of environmental friendliness based only on energy use or material waste (Demmer et al., 2018; Fera et al., 2016). The ecological impact of different AM machines, showing that they can vary by up to an order of magnitude, and that the machining of plastics generally requires no lubrication (DebRoy et al., 2018).

AM is more efficient than traditional manufacturing in terms of resource consumption, because a final product includes a higher proportion of the raw materials. Traditional manufacturing, such as injection molding (IM), uses large amounts of raw material for the likes of mold forms that are not parts of the final products. If the same raw materials are used in both traditional and AM methods, AM clearly has the advantage in terms of efficiency (see Fig. 2.4).

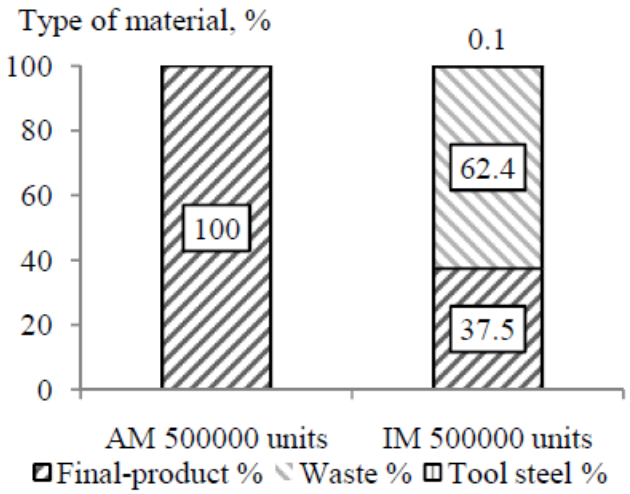

Figure 2.4: Comparison between AM and injection molding (IM) processes for 500,000 units of production volume (Ferrar, Mullen, Jones, Stamp, & Sutcliffe, 2012)

Considering the energy consumption per unit produced, AM processes always use more energy than traditional methods such as injection molding at higher production volumes. However, AM has the advantage in terms of energy usage at low production volumes. The crossover point of energy versus production volume depends significantly on the raw material choice and product geometry. Analyses of energy consumption have shown that most of the energy used in AM is used in the creation of the final product, whereas in traditional manufacturing, only a fraction of the total energy is used for the production of the final product (Kellens, Mertens, Paraskevas, Dewulf, & Duflou, 2017).

It is always true that different manufacturing methods produce different properties when applied to any one material; for instance, the microstructure and properties of wrought 316L are quite unlike those of cast 316L. Therefore, it is also logical to expect SLM parts to differ from traditional parts in the corresponding material. Although the differences are generally predictable, they can be surprising, as illustrated by the following examples

1. The object fabricated using laser based techniques generally has finer grain sizes than the object that fabricated by casting. This is due to the rapid solidification in the laser based techniques that happened as a consequence of the immediate elimination of the heat when the laser beam moves, and also from the heat conduction from the melted area to the powder bed and the metal. Figure (2.5) illustrates the micrographs of stainless steel object fabricated using EOS M280 system and an object with the same material fabricated using casting. By comparison between the two micrographs, it is obvious that the grain size of the SLM object is finer than cast object (Olakanmi, Cochrane, & Dalgarno, 2015).

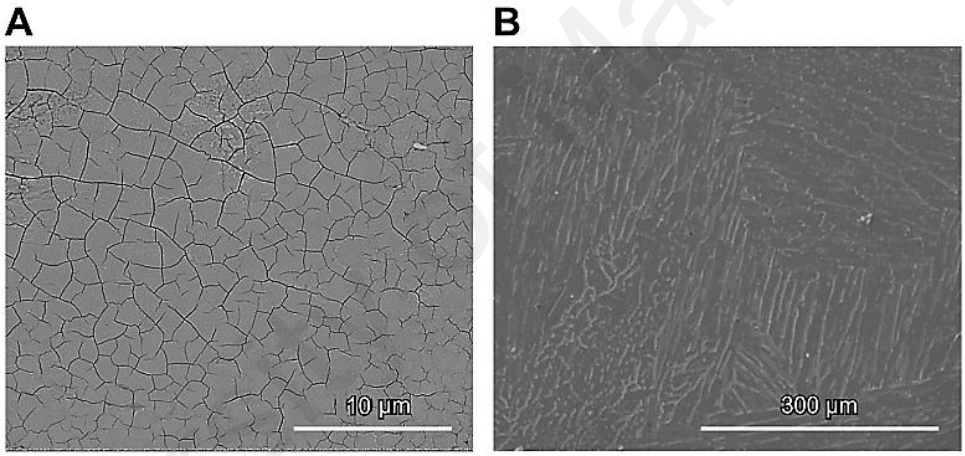

Figure 2.5: microstructure comparison between stainless steel fabricated by (a) SLM, (b) casting (Sames et al., 2016).

2. The kinetics of the material in SLM objects could be different than traditional fabricated object. For example, the strength and hardness of casted 17-4 stainless steel objects could be enhanced using heat treatment at 900^0F. However, this heat treatment was examined on an object fabricated using laser sintering and the results shows a decrease on the tensile strength which was unexpected results. This behavior appears as a result of the duplex-type steel structure formation as

well as the austenitic and ferritic phases the forms as a result of the rapid melting and cooling (Sarkar, Siva Kumar, & Kumar Nath, 2017).

2.5 Advantages and Disadvantages of Additive Manufacturing

The development of laser-based AM offers multiple advantages and the possibility of industrial applications. Generally, the primary advantages offered by AM processes are the ability to create complex geometries that cannot be formed by traditional manufacturing processes and the lack of necessary auxiliary devices and tools. From an industrial standpoint, these advantages present several pivotal implications.

Individual components are often manufactured in different factories with special tooling and are then shipped to assembly sites. With AM, parts are formed without specialized tools, allowing the on-site production of many parts and the elimination of the need for supply chains. Furthermore, as AM is also capable of printing interlocking parts, AM also decreases the number of parts per component and the need for assembly.

Regarding product distribution, AM could fundamentally change the objects that are distributed. AM products are arguably based on the digital file for the product model; therefore, the file, rather than the physical product, could be distributed. With a digital file, any user with access to the appropriate AM hardware could produce the physical product (Campbell & Ivanova, 2013). From a logistical standpoint, AM allows manufacturers to create parts that are not ordered often, but which must conventionally be warehoused, on an as-needed basis, thus reducing warehouse load. Given the capabilities of AM, these parts could be created at much lower volumes, thereby decreasing the cost of storing many uncommon spare parts. The current state of AM technology is such that several successful applications can already be found, including in custom orthodontics, hearing aids, prosthetics, and other medical devices, since AM processes can be used to form specialized parts.

However, despite the promise of AM, the inherent limitations of AM must be acknowledged. The most notable issue, which relates to industrial applications, is the time required to complete the build, which is an inherent effect of the layer-by-layer construction of the product. For instance, the formation of a small cube could take hours when using AM, but could be completed in minutes with injection molding. Furthermore, metal AM products lack the necessary consistency in the desired properties for commercial distribution. For these reasons, AM requires further advancements in efficiency and process control before it becomes a viable means of mass production (Simchi, Petzoldt, & Pohl, 2003).

2.6 Material and Processing in SLM

2.6.1 Stainless steel grade 316L

The feedstock powder of the SLM method consists of very fine particles. The size of the particle usually in the range of 20 to 35 μm. The majority of the SLM manufacturers also provide metal powder which has the best performance for the machines they produce. The 316L stainless steel is a metal that has high resistance to the corrosion. The chemical composites of the stainless steel are illustrated on table (2.1) where each element is represented as a percentage on the material composition.

Table 2.1: chemical composition of 316L stainless steel

Element	Content percentage
Fe	Balanced
Cr	16 – 18
Ni	10 – 14
Mo	2 – 3
C	0.03
Mn	2
P	0.025
S	0.03
Si	1

2.6.2 Feedstock Powder Properties and Characteristics

The powder characteristics and properties must be considered as they influence the SLM process and densification kinetics. Table 2.2 summarizes some of these major properties, some of which are interrelated. For example, the size of the powder as well as the distribution both affect the melt viscosity and the flow rate of the powder (Chang, Gu, Dai, & Yuan, 2015). Finer particles absorb more energy from the laser beam, consequently increasing the temperature of the particles and kinetics of densification, because the powder presents a larger surface area than one with coarser particles. Finer particles can also fill voids and therefore increase the powder density, producing higher solidification rates and finer microstructures (Rajabi et al., 2009). However, the flow of nanopowders is often inferior; nanopowders often agglomerate, increasing the optical reflectivity of the powder bed and thereby decreasing the energy absorption and densification kinetics (Yang & Evans, 2004).

Table 2.2: The properties of the powder and characteristics affect AM process

Property type	**Examples**
Chemical properties	alloy composition, oxygen and carbon concentration, reaction enthalpy, oxidation potential
Granulomorphometric characteristics	particle size and distribution, particle morphology, roughness, powder flowability
Rheological properties	viscosity and surface tension
Mechanical properties	elastic modulus, yield point, tensile strength
Thermal properties	conductivity, specific heat, melting temperature, thermal expansion
Optical properties	Reflection and absorption ratio, optical penetration

2.6.3 Process parameters

Figure 2.6 illustrates the SLM processing parameters that have a major influence and which must be considered. One common means of considering combined multiple interdependent process parameters in SLM utilizes the Andrew number (Raghunath & Pandey, 2007), which can easily be expressed as an energy density E, given by $E = \frac{P}{vst}$ (Lavernia & Srivatsan, 2009) where p is the laser power, v is the scanning speed, s is the hatch spacing, and t is the layer thickness. In addition, the use of different scanning patterns for the laser can produce different microstructures and properties (e.g., density, hardness, residual stress, etc.). By varying E and the scanning pattern, it is possible to improve the densification, microstructure, and mechanical properties of the SLM product.

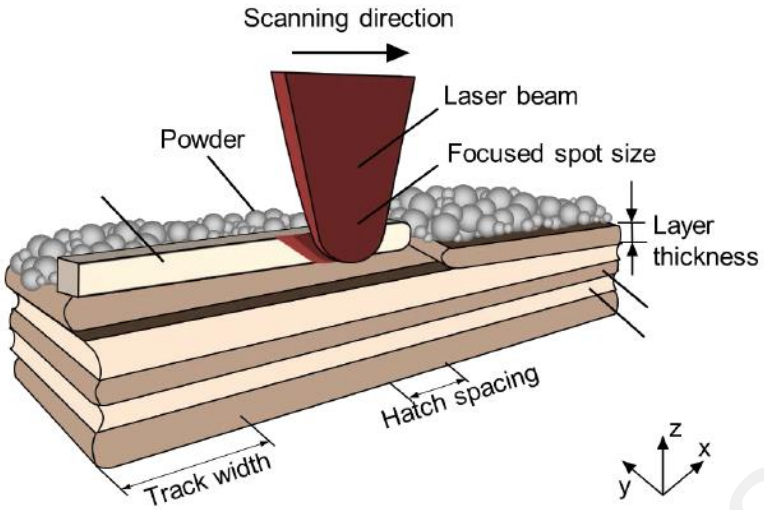

Figure 2.6: diagram illustrates the main process parameters on SLM.

In addition to the mentioned parameters, modifying the chamber environment have an important effect on the residual stresses. The most important parameter that need to be considered is the inert gas. The use of noble gas during the SLM process prevents the oxidation and minimize the gradients of the temperature in the powder bed (Gu & Shen, 2008). The effect of present of Oxygen in the chamber environment and how to eliminate it was investigated and the experiments revealed that passing a noble gas inside the chamber during the SLM process prevents the oxidation between the built layers of the object and keeps more uniform temperature through the process (Gu & Shen, 2008) . (Ferrar et al., 2012) studied the effect of inert gas flow on the performance of SLM process. Results shows that the use on insufficient flow rate will affect the mechanical properties of the built object. In addition, the experiment shows that the variation of the inert gas uniformity has a direct impact on the density and compression strength of the objects tested. Moreover, the use of insufficient inert gas during the process cause the appearance of mechanical defects on the microstructure of the built object.

2.6.4 The mechanism of solidification and the microstructure of the melt pool

Because of the high scanning speed during SLM process, the laser beam and the powder interact together for a small period of time. This action leads to fast melting of the powder and quick solidification (see figure 2.7) (Kruth et al., 2007). Many physical phenomena are included in SLM method such as phase transformation, heat transfer, absorption and reflection, chemical reactions and surface tension (Tan, Wong, & Dalgarno, 2017). The geometry of the melted pool as well as the rate of cooling influence the microstructure and the grain growth of the fabricated object, while creating a temperature gradient across the melt in order to generate surface tension that keep the flowing of the melt in a radial direction (Guan, Wang, Gao, Li, & Zeng, 2013). The Marangoni flow strength as well as the depth of the convection is basically affected by decreasing the scanning speed (see figure 2.7). There are several advantages when obtaining the Marangoni flow. For instance, increase chemical homogeneity, metastable phase formation, extension of solubility and fine microstructure.

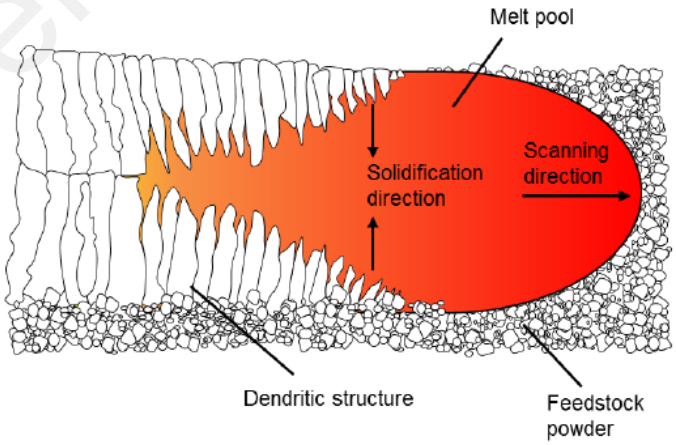

Figure 2.7: Solidification in SLM process

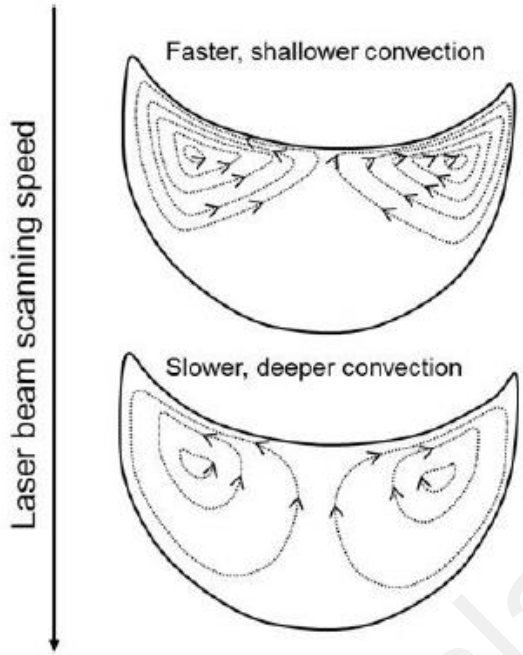

Figure 2.8: The influence of scanning speed on the depth and strength of convection during SLM process.

The microstructure types of an object fabricated using SLM can be classified into two categories. One of which has large grain sizes that are arranged in columns as formed by the epitaxial growth; this occurs when the growth of the grains following the path of the maximum thermal gradient. In SLM, during successive layer deposition, the previous layers are re-melted, which causes each new layer to adopt the same crystallographic orientation as those below; this is the "epitaxial growth mechanism.". The other category of the microstructure types has finer grain sizes that growth in the direction of the melted pool center. The type of the melt solidification can be easily altering by changing the energy density (E) of the process. Figure 2.9 shows an example of optical and SEM micrographs of as-built SLM 17-4 stainless steel, which exhibits a unique microstructure. The optical micrograph shows a microstructure typical of an SLM-processed material, featuring overlapping bowl-shaped features that result from the solidification of the melt pool after

each laser scan. The strong grain orientation in the SEM image indicates that solidification occurs for crystals growing perpendicularly to the close-packed austenite planes. The clear, simultaneous appearance of the two microstructures (bundles of columnar grains as well as fine equiaxed grains cutting through the boundaries of the melt pool in the building direction) is observed.

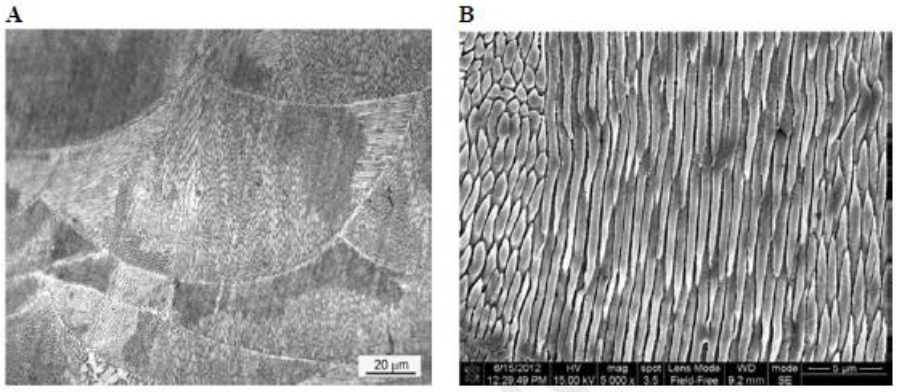

Figure 2.9: Microstructure of stainless steel (A) optical microscope image, (B) SEM image (Liverani, Toschi, Ceschini, & Fortunato, 2017).

2.6.5 Material textures

The directional solidification of objects produced by SLM, show textures. The scanning technique that identifies the solidification direction is the main parameter that influence the texture. For instance, a strong texture appears for unidirectional scanned cubic metals that growth in a perpendicular angle to the scanning direction (Sarkar et al., 2017). On the other hand, in case of bidirectional scanning strategy is employed, where the zigzagging patterns are applied in the scanning procedure, weak texture will be produced since the columnar structure of the grains is demolished.

2.6.6 Grain size

The SLM objects usually have finer microstructures when comparing to the objects created using traditional manufacturing methods (Guan et al., 2013). Because of the limited growth time for the grains as well as rapid solidification, the sizes of the grains for objects fabricated using SLM technique are fine. By changing process parameters, however, the microstructure of the SLM object may be enormously altered.

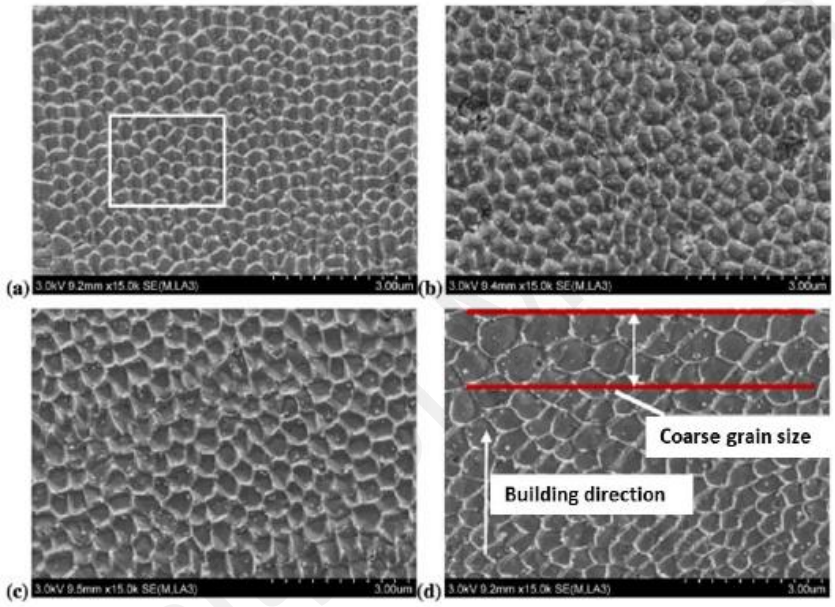

Figure 2.10: SEM images shows the cellular dendrites of 316L object produced at different parameters (a) 105.7 J/mm^3, 1.2 m/s; (b) 152 J/mm^3, 1000 m/s; (c) 155.5 J/mm^3, 800 m/s; (d) 187 J/mm^3, 700 m/s (Guan et al., 2013).

Figure 2.10 demonstrates the microstructure of 316L stainless steel object fabricated using SLM at different energy densities and scanning speeds. The images appear that the dendritic arm spacing increases when the scanning speed of the laser decreases. Whereas by increasing the energy density, the dendrite spacing increases. The reason behind this behavior is that at low scanning speed the rate of cooling is relatively low, also for high energy density the melted pool temperature is high that provides more time for the grains to growth.

2.6.7 Defects.

The consolidation in the laser based methods is basically depending on some parameters such as temperature gradient, surface tension, and gravity. SLM objects may experience a few popular defects such like the appearance of porosity. There are three types of pores that usually appears on the SLM objects which are large pores, micro-pores and spherical pores that may occurs due to inefficient melting, reduced feeding in the interdendritic regions and trapped gas respectively (Patterson, Messimer, & Farrington, 2017).

Another kind of defects appears on the SLM object because of the inability of the melted material to wet the substrate underneath, this kind of defects known as balling (Li R, 2012). Balling phenomenon extremely reduces the quality of the SLM process and increases the porosity density (Maurice DR, 1990).

Because of the process feature of the SLM, this method may bring out residual stresses due to the huge temperature gradients. As the melted layer solidifies and shrinks, the object is subjected to tensile stresses. Moreover, tensile stresses in the deposited layers also created due to the strains on the substrate which added to the residual stresses (Paul et al., 2007). The residual stresses cause some deformation through the built object which effect the object quality. The rapid cooling process in SLM increase the deformations and defects on the build object, and extremely reduce the tensile and fatigue strengths (Zhang, Dembinski, & Coddet, 2013).

Objects that fabricated at low energy density usually suffer of bad wetting and spheroidization. The density of the fabricated object is enhanced when using high energy density, however, the tracks of the laser beam are cut off, being present like short strips. The medium energy density generates continuously tracks in all layers (Kempen, Thijs, Humbeeck, & Kruth, 2014).

Figure 2.11 illustrates the effect of the energy density on the porosity. The figure bellow demonstrates the relation between the average density of 316L stainless steel calculated using the principle of Archimedes and the energy density of the laser. Generally, a wise energy density increment leads to improving in densification but the unreasonable energy density may lead to reduced viscosity and creates residual stresses that cause cracks.

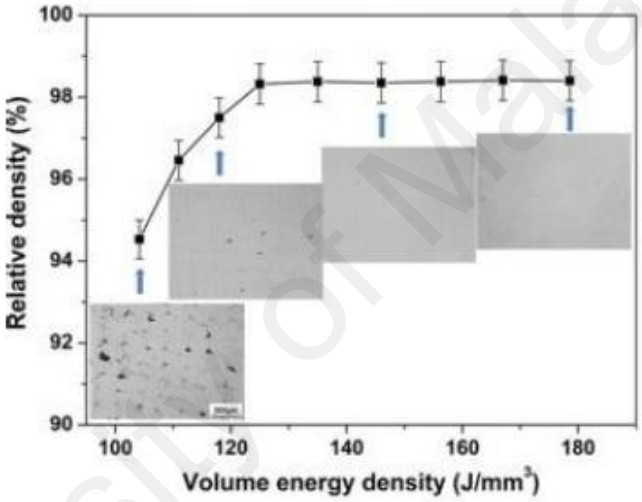

Figure 2.11: Variation in relative density of SLM-processed 316L parts under various energy densities (Kempen et al., 2014).

The SEM images that illustrated on figure 2.12 was taken for 17-4 stainless steel samples that were fabricated using the specific process parameters. The process parameters for the three samples were 195 W and 1200 mm/s, 95 W and 389 mm/s, and 70 W and 287 mm/s respectively. The porosity on these samples were notably higher than other samples were fabricated under different process parameter. In the first image where the process parameters are 195 W and 1200 mm/s, the energy density is enough to completely melt the powder of stainless steel. However, as seen in the second image, the

laser scan tracks show discontinuity from the balling phenomenon. The process parameters of this sample were 95 W and 389 mm/s laser power and scanning speed respectively. As can be seen in the second and third SEM images where the laser power were 95 W and 70 W which is low that causes for insufficient melting with limited liquid phase formation.

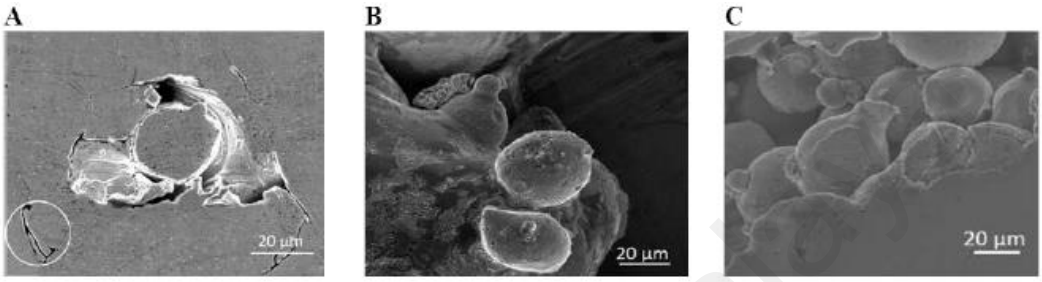

Figure 2.12: SEM images of pore morphology using (a) 195 W power and 1200 mm/s scanning speed, (b) 95 W power and 389 mm/s scanning speed (c) 70 W power and 287 mm/s scanning speed (Kempen et al., 2014).

2.6.8 Inert gas and defects

In addition to parametrizing the basic input parameters for the process, modifying the chamber environment seems to have a positive effect on the residual stresses. These controls primarily consisted of chamber temperature control, using inert gases to prevent oxidation and reduce temperature gradients in the powder bed. (Jia and Gu, 2005), (Dai and Gu, 2006) and (Dadbakhsh et al., 2008) looked at the effect of having oxygen in the environment during printing and ways to eliminate it. Dai and Gu and Dadbakhsh et al. suggested running an inert gas through the powder bed during the process to prevent oxidation between the layers of the part and produce a more uniform temperature throughout. (Ladewig et al., 2012) examined the use of the inert gas to deal with metal splatter and to flush out process by-products and trash. (Buchbinder et al.,

2012) and (Mertens et al., 2015) examined the ways to effectively pre-heat the powder and build plate to reduce the likelihood of stresses

CHAPTER 3: METHODOLOGY

3.1 Samples specifications

The as received samples of 316L stainless steel has the following dimensions; the length is 9.6 cm, width is 1 cm, thickness is 2 mm and the middle section width is 0.5 cm Figure 3.1 illustrates the sample dimensions.

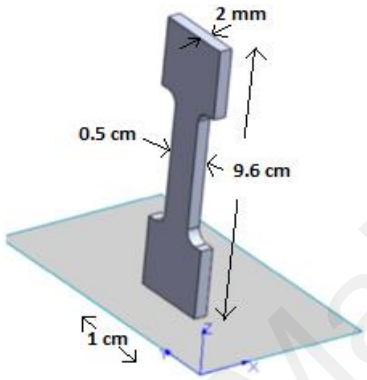

Figure 3.1: systematic drawing of the sample illustrating its dimensions

The composition of the stainless steel as provided by the manufacturer includes the following contents that stated in table 3.1.

Table 3.1: the chemical compositions of 316L stainless steel

Element	Cr	Ni	Mo	P	C	Si	Mn	Fe
Wt%	16 - 18	10 - 14	2 - 3	0.045	0.03	1	2	Bal

The metal powder used in the manufacturing of the samples was produced using gas atomization. The benefits of this technique is provided in section (2.2). The particle size of the stainless steel powder was 20 – 35 micro meter.

The total number of samples used in this study is two as shown in figure 3.2.

Figure 3.2: 316L stainless steel samples used in this project

The samples were fabricated using SLM technology under different process parameters as shown in table 3.2. The laser power used in the manufacturing process was 360 W for both samples while the scanning speeds were 250, and 510 mm/s respectively to study the effect of scanning speed on the mechanical properties. At the beginning of the manufacturing process, the Argon gas was fills the chamber. Near to the end of the process, however, the Argon gas had run out and the process continued without the inert gas. Table 3.2 illustrates the process parameters for all samples.

Table 3.2: Process parameters of the two samples used in the study

Sample Number	P (W)	V (mm/s)
1	360	250
2	360	510

The reason of using different scanning speed is to illustrates the effect of energy density on the tensile strength of the samples.

The fabricating orientation was vertical as shown in figure 3.3. The layer thickness of the samples was 50 µm.

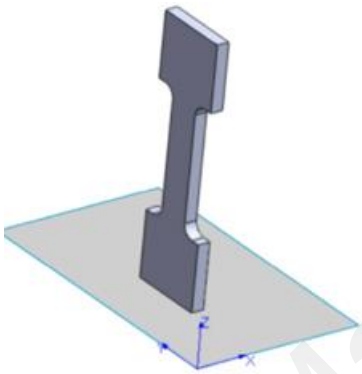

Figure 3.3: Manufacturing orientation of the samples

3.2 Tensile Test

Prior starting the tensile test for the samples, the precise dimensions of the sample such as the length, width, thickness and cross section were measured by using the micrometer and all these measurements were recorded before starting the tensile test. The tensile test was performed using Instorn Testing Machine available at the University of Malaya. The set-up of the tensile test follows the standard of ASTM E8 for metal testing. Figure 3.4 shows a picture for the machine used in the tensile test.

Figure 3.4: Instron tensile test equipment

The machine consists of dual vertical clamps that are used to fix the sample in the position of the test. The tensile testing machine function by comprising two clamps. The first one is the bottom clamp which is the fixed clamp. The second is the upper clamp which is the moving one. This design of having two clamps in which one of them is moving and the other is stationary grants the machine to better control the motion and the velocity through controlling a single clamp. All samples were tensile tested by the use of the same displacement rate which is 1 mm/minute. The samples were placed in a vertical position and at the same time the samples are parallel to the direction of the testing that will provide more precise results, see figure 3.5.

; 

Figure 3.5: Sample test in progress

The method of the tensile test was done by the use of Bluehill software. After finishing the test and the sample broke, the Bluehill software is able to produce a file that contains all the information needed from the experiment. The gathered information includes: Load, elongation, tensile stress, strain and time. The information in the excel sheet was used in analysis of the tensile properties of the samples.

3.3 Microstructure and porosity Observation

The microstructure of the samples as well as porosity observations were done using available optical microscope and scanning electron microscope (SEM) at mechanical engineering department, University of Malaya Figure 3.6.

Figure 3.6: SEM equipment, CAREF lab (UM)

To achieve better observation, the samples were prepared prior starting the observations. The preparation includes the cutting of the sample into three parts to the desire length which less than 15 mm. The parts represent the lower, middle and upper part of the samples number 1 and 2. Then the samples were mounted. The mounting makes the grinding and polishing easier since it became easy to catch the sample during the process, figure 3.7.

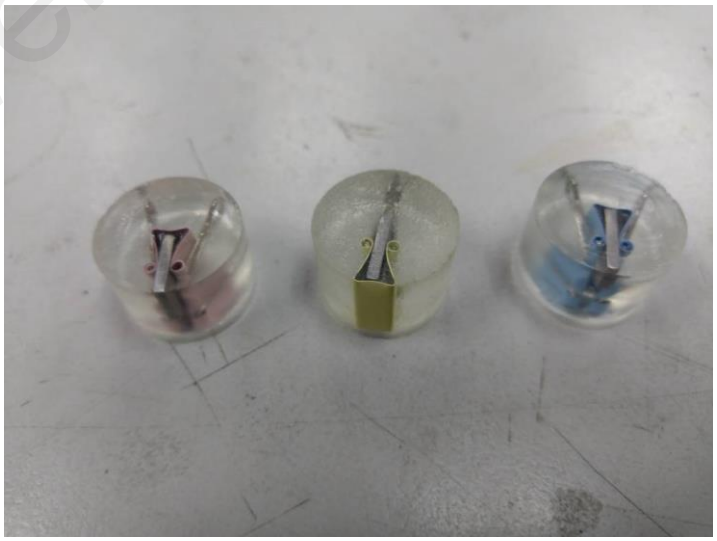

Figure 3.7: Mounted samples.

After that the samples were grinded using different sand papers sizes starting from P80 and up to P2000, see figure 3.8. The grinding helps to soften the surface of the sample and remove scratches that occurs during the cutting process. Polishing also was performed for the samples using Alumenia solution 0.03 nm particle size in order to achieve a very smooth surface. Finally, after polishing the samples were etched.

Figure 3.8: Grinding and polishing machine.

Then the samples were placed inside the SEM machine for porosity observation. Figure 3.6 shows the SEM machine used in the observation. Images were taken in different regions at the surface starting from the bottom and going to the top. The captured images vary in terms of the magnifications from 230x and up to 1550x to obtain better images of the surface characteristics. An optical microscope was used for microstructure observation for all samples.

3.4 Nanoindentation

Nanoindentation was performed to measure the hardness for different section of sample 2. The hardness analysis was done in nanoindentation lab at the University of Malaya.

Figure 3.9: Nanoindentation equipment available at UM.

The machine uses Berkovich shaped diamond indenter head with diameter 100nm. The three samples were well prepared by grinding and polishing before starting the test. Figure 3.10 shows the sample placed in the machine chamber for nanoindentation test.

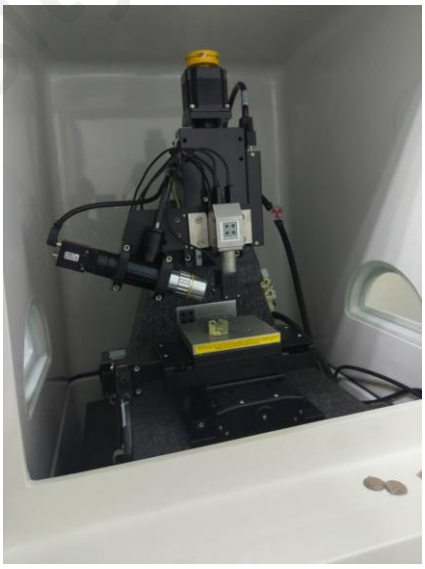

Figure 3.10: Sample placed in the chamber for nanoindentation test.

The samples used in this test have to be flat on both sides to ensure precise results. The force used in the test was 4 mN and the loading rate is 269 nN/s which need 15 seconds for loading and 15 seconds for unloading. Each sample was indented five times with spacing 50 µm between the indents which is equal to the layer thickness during production. The hardness was taken as the average of these measured results.

3.5 Micro hardness

The Vickers hardness of the SLM-processed samples was measured using a micro hardness tester at a load of 200 g and an indentation time of 10 s for a minimum of 5 indentations. All of the samples were ground and polished prior to hardness testing to obtain a uniform surface finish. Figure 3.11 shows the micro hardness machine used in this study.

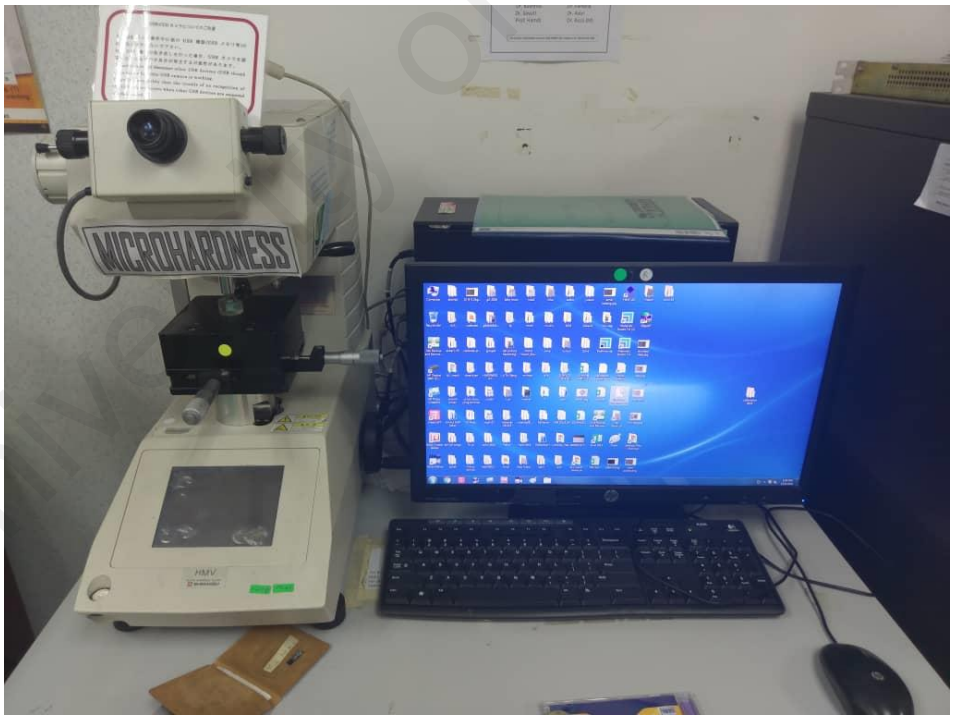

Figure 3.11: Micro hardness equipment used in this study.

CHAPTER 4: RESULTS AND DISCUSSIONS

4.1 Tensile test

The tensile tests were performed to evaluate the mechanical properties of the samples under static loading. As mentioned before, the plastic deformation of the sample under tensile stress is identified by using 0.2% offset technique, figure 4.1 shows an example of calculating the yield strength from stress – strain curve.

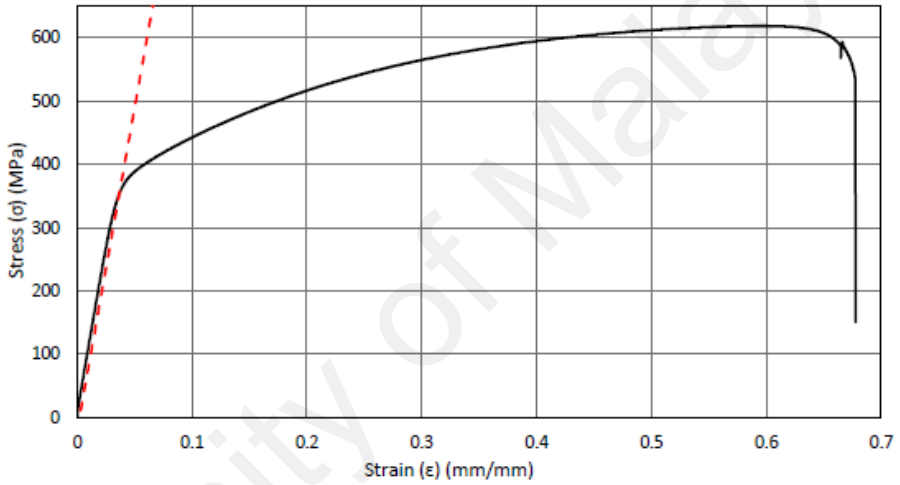

Figure 4.1: An example of identifying the yield stress using 0.2% technique

The yield strength (YS) is the value of the stress that indicates the end of the elastic region the beginning point of the plastic deformation. The maximum stress value on the stress – strain curve is known as the ultimate tensile strength (UTS). The elastic modulus (Young's modulus) can be extracted from the stress – strain curve. It represents the slope of the elastic region of the curve which is a linear relation. After the test was completed, the BlueHill software creates an excel file records all values collected during the tensile test such as tensile strain, tensile stress, extension and time. The collected data was used to evaluate the mechanical properties of the sample such as yield strength (MPa), ultimate strength (MPa), and modulus of elasticity (GPa). The stress – strain curve shows the

variation of the stress and evaluation of the strain through the tensile test procedure. The stress is represented on the vertical axis while the strain is represented on the horizontal axis. Figure 4.2 and 4.3 show the tensile results of the samples used in this study.

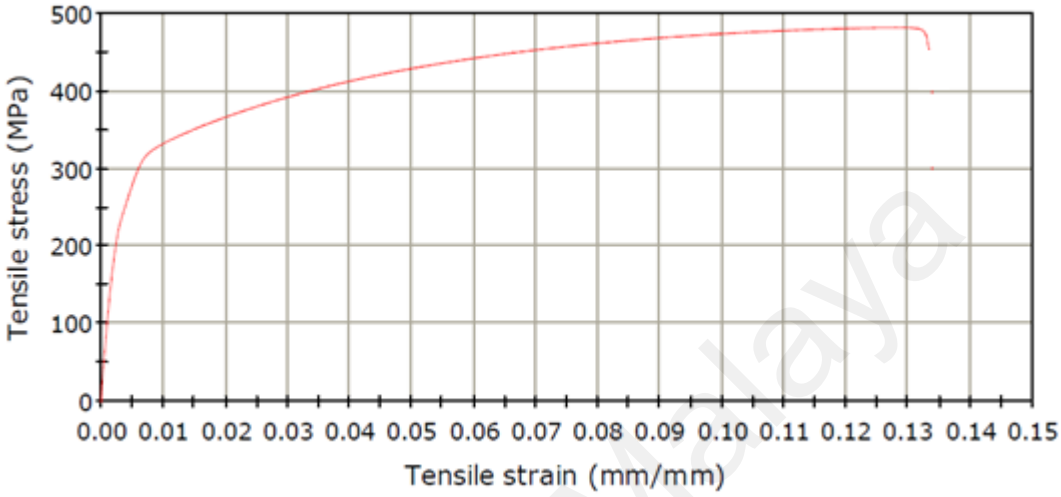

Figure 4.2: Tensile test result for sample1

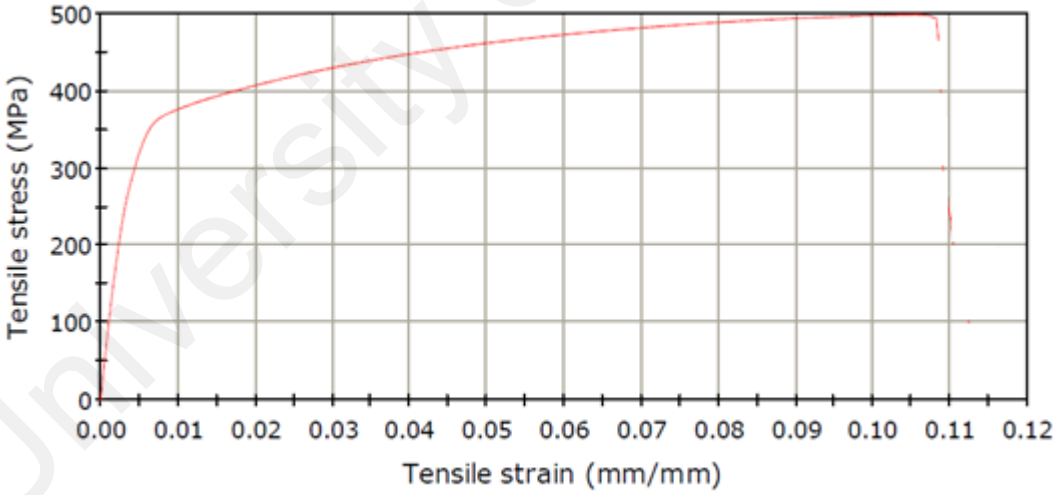

Figure 4.3: Tensile test result for sample 2

As can be seen in figures 4.2 and 4.3, the ultimate strength of the sample 1 that was fabricated using 250 mm/s scanning speed is 482 MPa which is lower than sample 2 that

produced with higher scanning speed. Moreover, the yield strength in sample 2 is about 323 MPa which is higher than sample 1 that was created using lower scanning speed. Table 4.1 summarizes the mechanical properties obtained from the tensile test.

Table 4.1: Yield strength, ultimate strength and calculated modulus of elasticity for both samples

Sample	Yield strength	Ultimate strength	Modulus of Elasticity
1	245 MPa	482 MPa	76.5 GPa
2	323 MPa	498 MPa	63.33 GPa

A comparative between the tensile test results is illustrated in figure 4.4 and 4.5

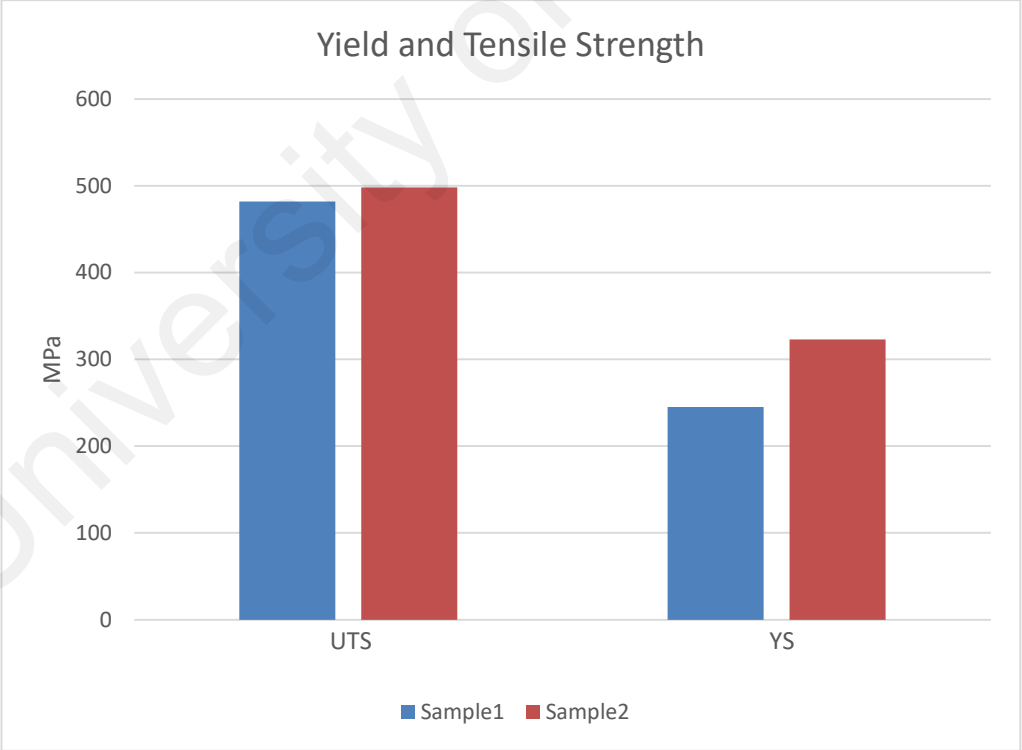

Figure 4.4: Ultimate tensile strength (UTS) and yield strength (YS) for both samples.

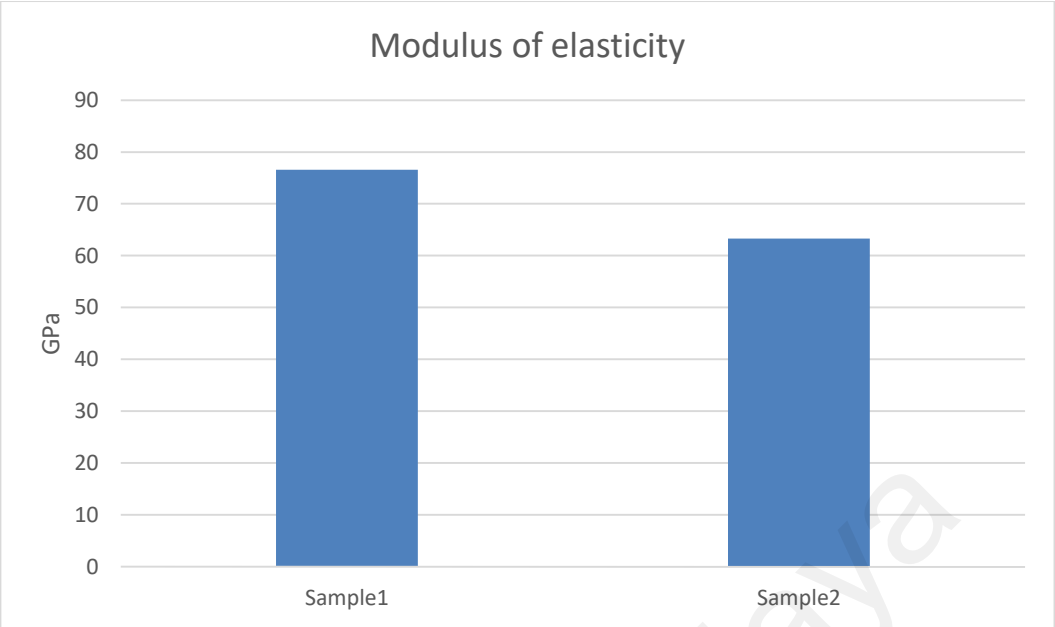

Figure 4.5: Modulus of elasticity for both samples

Figure 4.6 shows the samples after the tensile test was completed. It is interesting to note that the break of both samples did not occur at the middle of the specimen as expected but it occurred with shifted distance closer to the side that produced with lower concentration of Argon gas. This observation is clear for both samples. The reason behind this behavior is attributed to the high density of pores in this region that cause a load concentration that lead to this behavior.

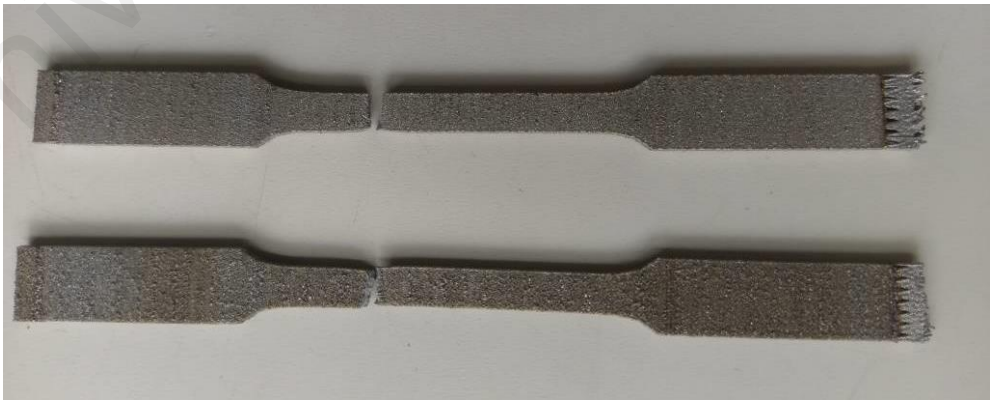

Figure 4.6: samples after break due to the tensile test

The variation of the mechanical properties in these two samples is referred to the use of different scanning speeds. In this case, since the Argon gas run out at the end of the manufacturing process, there is a great possibility to form oxides in between the built layers. As the scanning speed increases, the chance of oxide formation is reduced due to the lack of time. Oxides between the built layers causes defects and cracks which cause a damage in the mechanical properties of the built object.

4.2 Microstructure

The microstructure and porosity observations for both samples was performed using optical microscope and SEM machine. The samples were cut into three sections in the workshop. The sections represent the lower, the middle and the upper part of the sample (see Figure 4.7).

Figure 4.7: Cut sections for both samples.

Section 1 represents the lower part of the sample where the Argon gas was presents during the manufacturing process. Section 2 is the middle part. Section 3 is the upper part

of the sample where the Argon gas run out during the manufacturing process. In this way it is possible to analyze the effect of Argon gas on the microstructure of the fabricated object. Results of optical microscope observation for sample 1 and 2 are illustrated in figure 4.8 and 4.9 respectively.

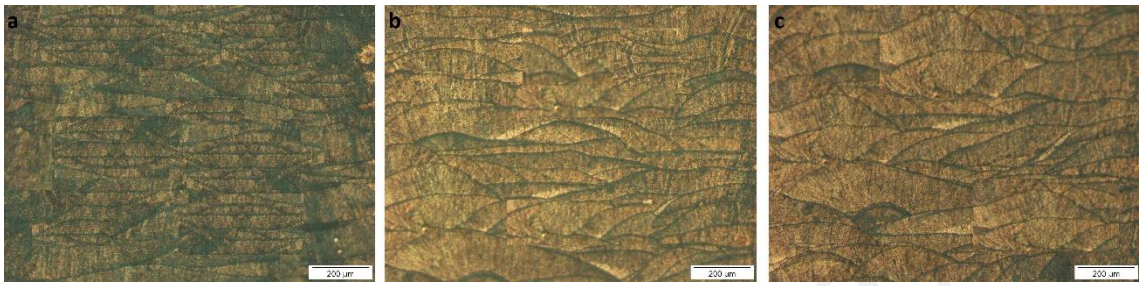

Figure 4.8: Microstructure of the three sections of sample 1. (a) section 1, (b) section 2, (c) section 3.

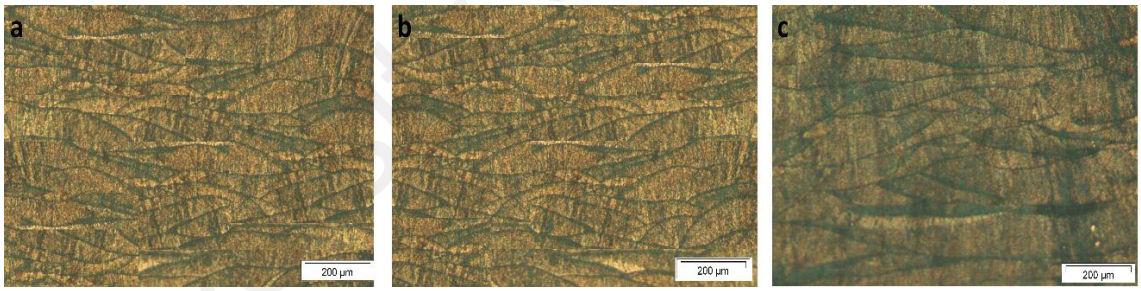

Figure 4.9: Microstructure of the three sections of sample 2. (a) section 1, (b) section 2, (c) section 3.

Microstructure observation of sample 1 and 2 shows that; section 1 and 2 has almost the same grain size. However, in section 3 were the argon gas was absence, the microstructure shows irregular sizes of the grains along the cross section. The inert gas keeps the required atmosphere for efficient manufacturing process such as keeping a uniform temperature through the process. The absence of the inert gas causes a non-uniform and asymmetric temperature gradient as well as local cooling rates that will lead

to different cell sizes increasing the heterogeneity in the laser melted steel sample as can be clearly seen in section 3 for both samples.

4.3 SEM / EDS analysis

Results of the SEM observations are illustrated in Figure 4.10. and 4.11 respectively The SEM images show the microstructure of the section 1, 2 and 3.

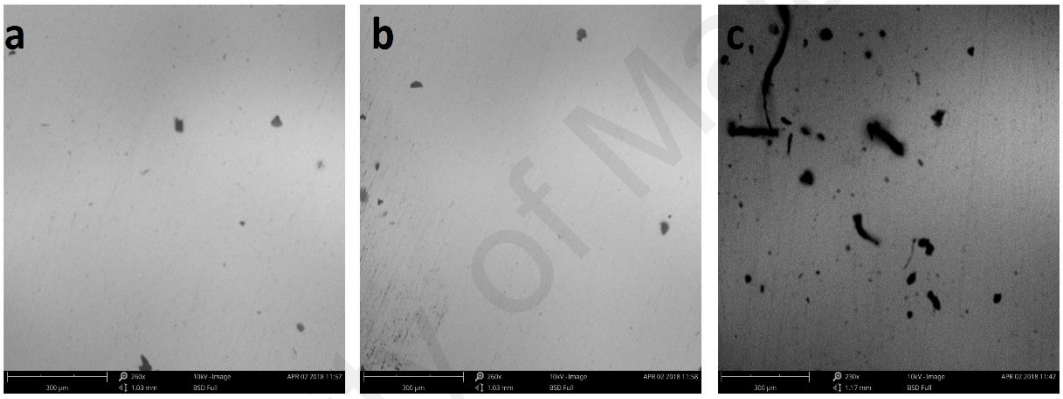

Figure 4.10: Microstructure of the three sections of sample1 (a) Section 1, (b) Section 2, (c) Section 3.

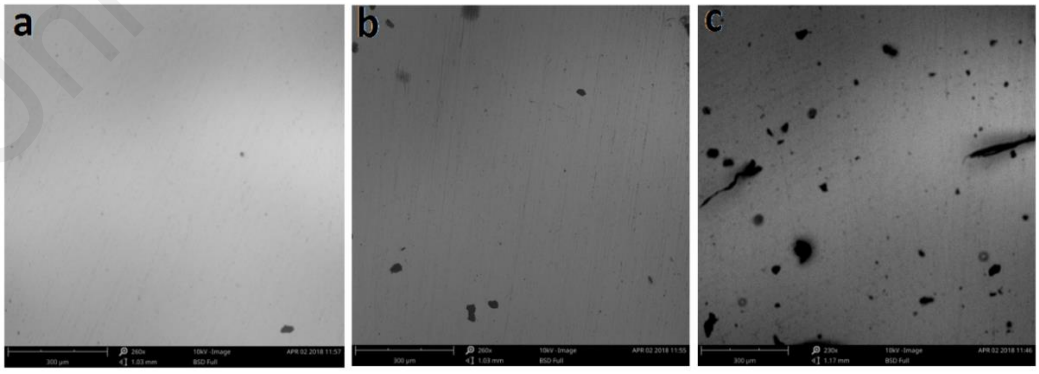

Figure 4.11: Microstructure of the three sections of sample 2 (a) Section 1, (b) Section 2, (c) Section 3.

As can be clearly seen in the figures, section 1 has a smooth surface with very few pores across the surface. The porosity density is increased on the other sections specially on section 3 where the Argon gas was run out.

A closer look for the pores can be found in Figure 4.9 which shows the pores for section 3 at 1550X magnification. Overall, it can be seen that pores size is ranging from 20 - 50 µm.

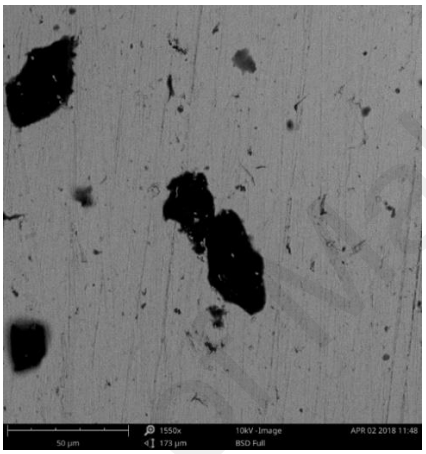

Figure 4.12: Porous in sample 2 section 3 with 50 µm size

As can be seen in Figure 4.9 that the pores are relatively big in this section since the manufacturing process performed with the absence of the Argon gas.

The inert gas is not only used to eliminate oxidation through the manufacturing process, but also employed to remove vaporized powder (condensate) from the laser path that would have a negative effect on the properties of the laser beam such as energy and spot diameter. effecting these parameters will lead to insufficient melting process and heterogeneity which will cause defects and pores in the microstructure

The EDS spectra shown in Figure 4.10 and 4.11. The EDS spectrum for all samples exhibit various peaks pertinent to the elements composing the sample, namely, Fe, Cr, Ni, and Mo, beside a peak for oxygen in section 3 in both samples, suggesting that the

section contains oxides in between the layers. however, Section 1 and 2 for both samples did not show any present of oxides.

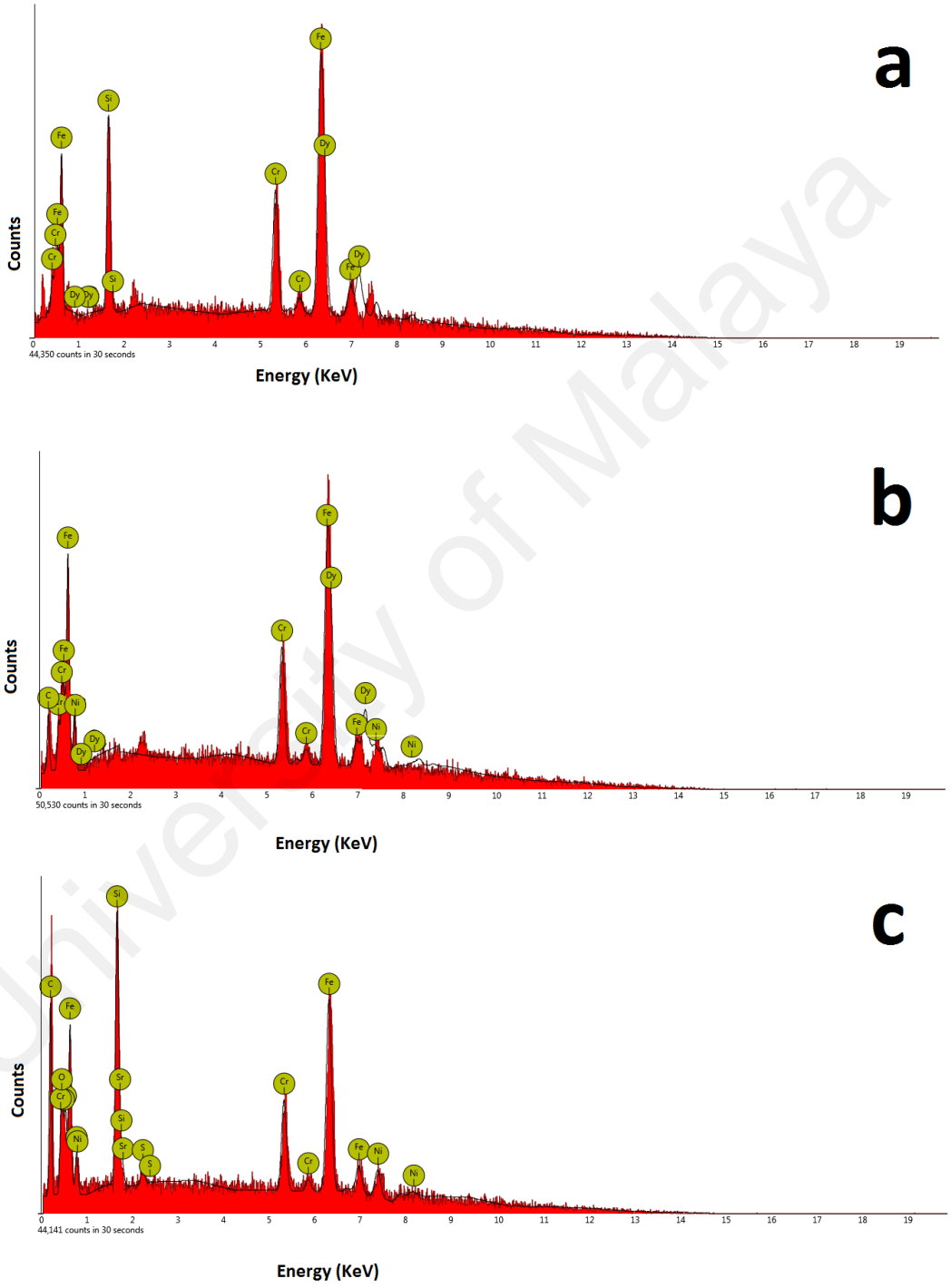

Figure 4.13: EDS analysis for sample 1 (a) section1 (b) section2 (c) section3

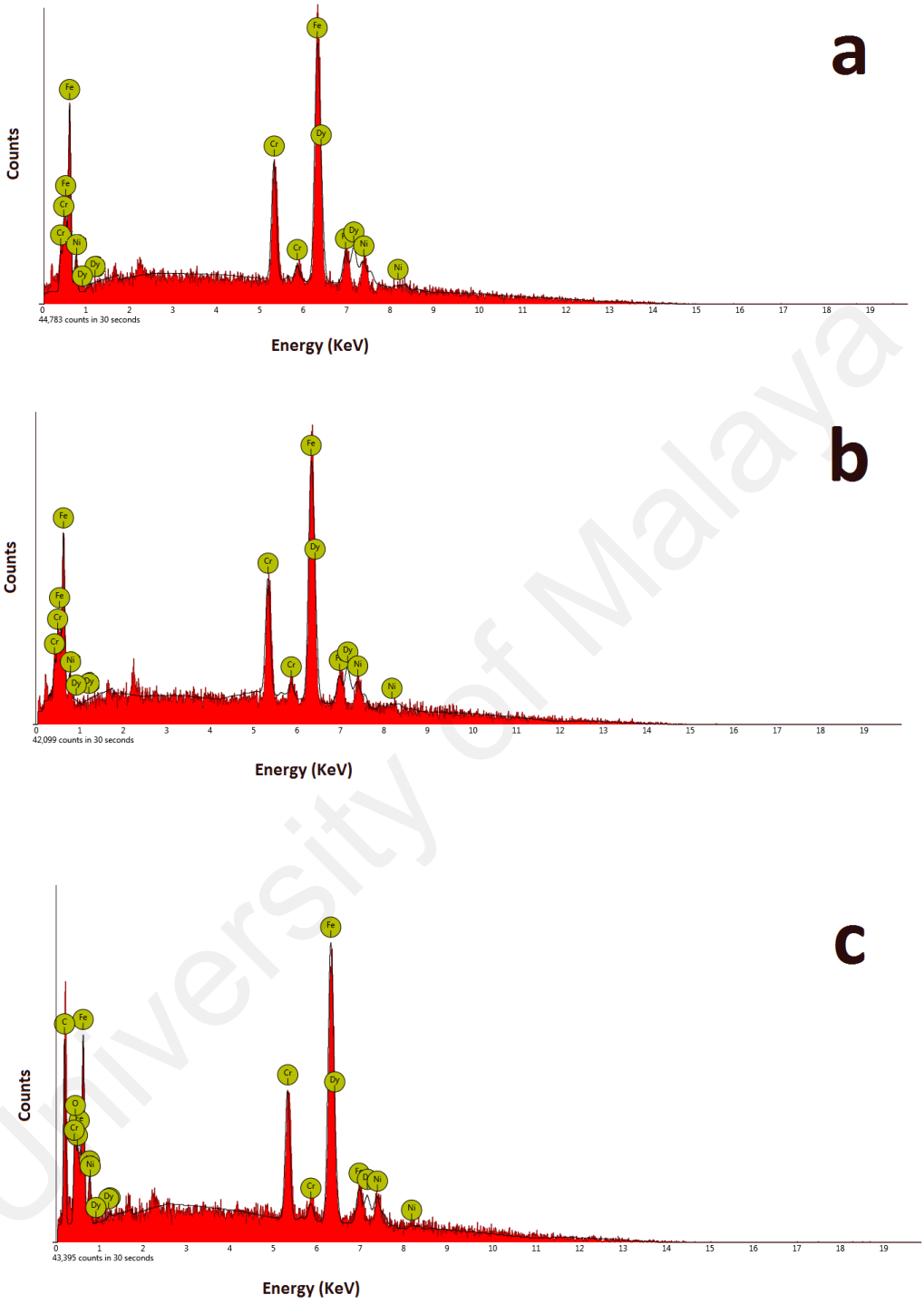

Figure 4.14: EDS analysis for sample 1 (a) section1 (b) section2 (c) section3

Present of oxygen in EDS spectrum show an evident of oxides presence in the built object. The oxides were formed in section 3 in both samples which were fabricated with absence of the inert gas. This results highlights the importance of the inert gas in eliminating oxide formation during SLM process.

4.4 Micro hardness

The micro hardness test was performed for all sections on both samples. The polished specimens were tested using Vickers micro hardness testing system available at University of Malaya. A load of 1.961N for a period of 10 seconds was applied to the specimens. The hardness was determined by recording the diagonal lengths of indentation produced as illustrated in Figure (4.9).

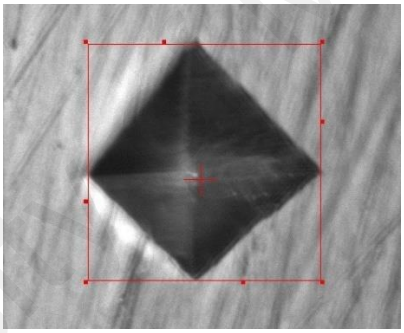

Figure 4.15: Determining the micro hardness by measuring the diagonal length

The test was performed on different five locations for each section and the average hardness value was taken as the hardness of the section. Results of this test are illustrated on table 4.2

Table 4.2: Micro hardness results for both samples at all sections.

Sample	Section	Micro hardness (HV)
Sample 1	Section 1	165
	Section 2	169
	Section 3	192
Sample 2	Section 1	172
	Section 2	178
	Section 3	205

There is a notable increment on the hardness in section 3 for both samples. This is due to the absence of the inert gas. The inert gas is employed to keep the appropriate atmosphere in the chamber to ensure efficient manufacturing process. The absence of this gas will lead to non-uniform temperature gradient and local cooling rates which will lead to form different cell sizes that will affect the hardness.

4.5 Nanoindentation

The nanoindentation testing was performed to evaluate the hardness for different sections of sample 2. The three sections of the sample number two was well prepared and flattened on both sides. Nanoindentation parameters used for all three sections were the same which are 4 mN, and 269 μN/s load and loading rate respectively. Number of indentation for each sample was 5 with 50 μm spacing distance between each two indentations. The nanoindentation software performs all calculations of the hardness. Also the software is able to represent the load vs depth of indentation in a graph.

Figures 4.16 – 4.18 shows the load – depth curve for the nanoindentation test.

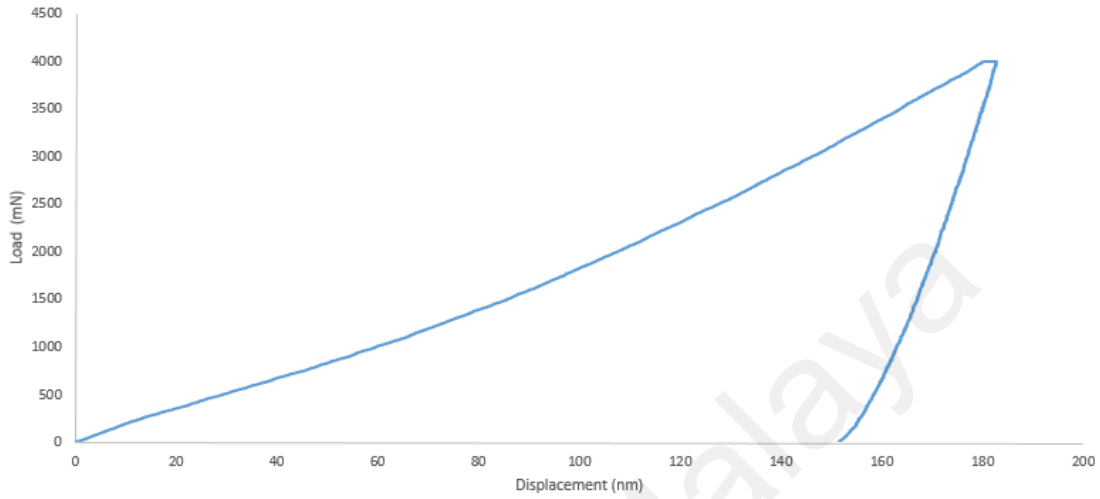

Figure 4.16: Load – displacement curve section 1 (scanning speed 510 mm/s)

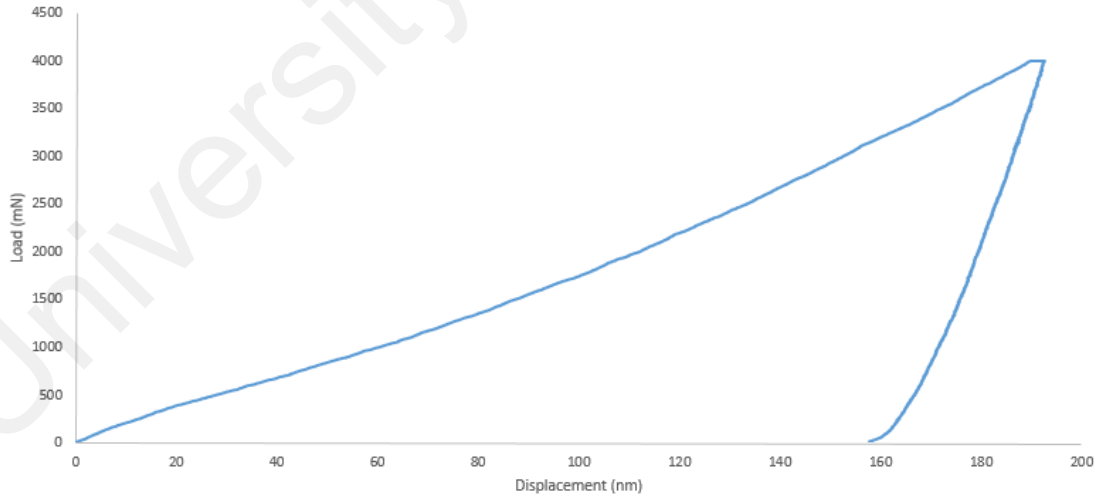

Figure 4.17: Load – displacement curve for section 2 (scanning speed 510 mm/s)

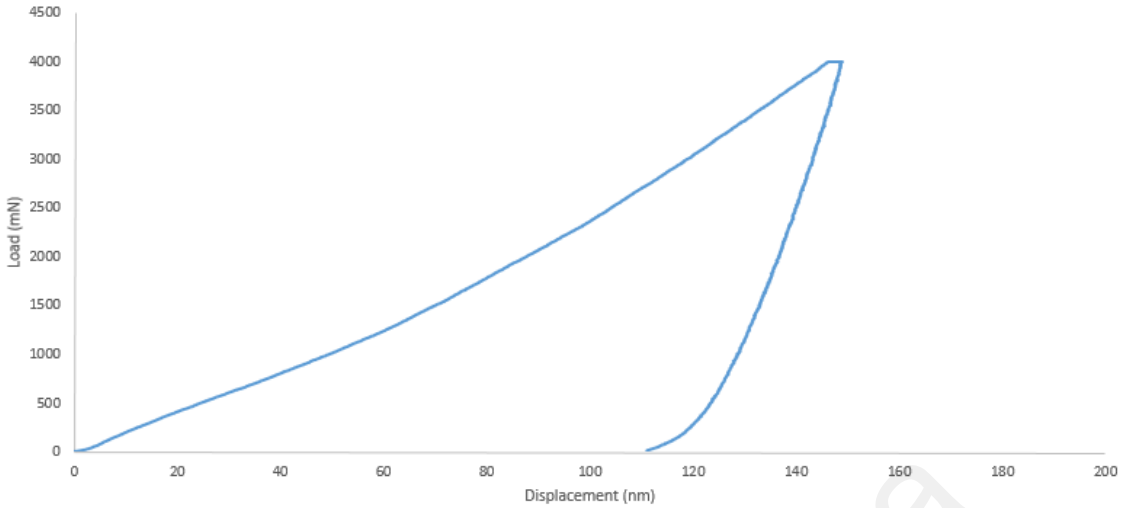

Figure 4.18: Load – displacement curve for section 3 (scanning speed 510 mm/s)

The hardness was measured for five indentations for each section. The average hardness for each section was calculated. Results appear that the hardness value for section 1 and 2 are almost similar. However, for section 3 that was fabricated with absence of the Argon gas, the average hardness was higher. The average hardness for section 3 was 4.527 GPa while it was 3.25 in the other sections. Table 4.2 summarizes the hardness results.

Table 4.2: hardness results sample 2 (scanning speed 510 mm/s)

Section	Hardness (GPa)
1	3.249611
2	3.2533166
3	4.527347

The nanoindentation results is illustrated in Figure 4.19. It is clear from the figure that section 3 which was produced without Argon gas shows higher hardness value than other sections.

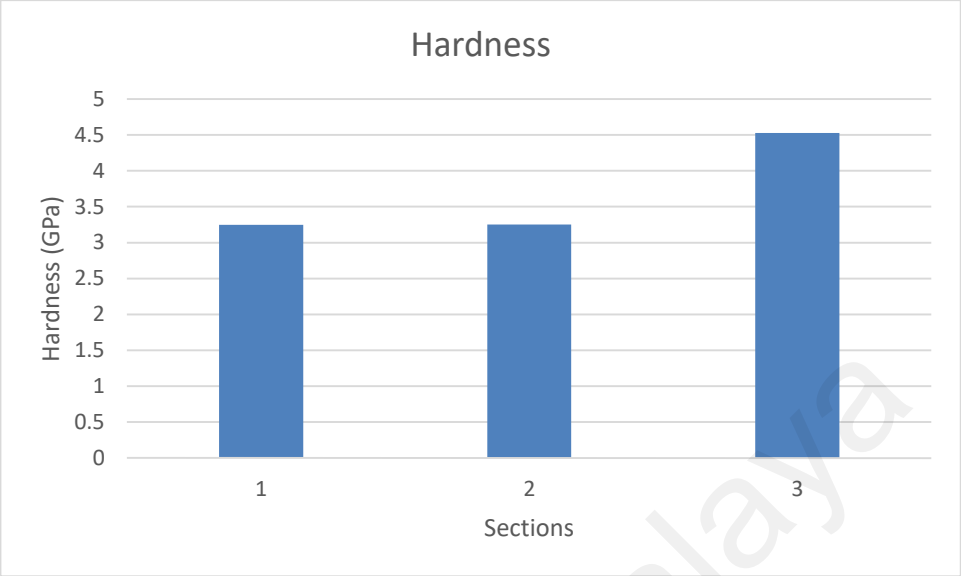

Figure 4.19: Hardness comparative between the three sections of sample 2

CHAPTER 5: CONCLUSION AND FUTURE WORK

5.1 Conclusion

The purpose of this project was to determine the effect of the inert gas on the microstructure and mechanical properties of 316L stainless steel object fabricated using SLM. For this purpose, a series of experiments were carried out to evaluate the mechanical properties and microstructure characteristics of the built objects. The samples used in this project were fabricated with present of Argon gas at the beginning, however, at the end of the manufacturing process the inert gas had ran out and the process continued without the inert gas.

The microstructure observation for the object shows high presence of pores in the section that was fabricated with absence of the inert gas. The microstructure of the other sections looks almost similar and there is no any notable difference.

The tensile test was performed to illustrate the effect of the scanning speed. For this purpose, two samples that fabricated using 250 mm/s and 510 mm/s scanning speeds were tested. By analyzing the stress – strain curve, it was determined that; the sample that fabricated with lower scanning speed has low ultimate tensile strength and yield strength while the modulus of elasticity higher. Even though it is able to determine the variation of these properties, the difference is still small. It is recommended to use more samples with different scanning speeds to see the significant effect. Moreover, after the tensile test was performed and the samples had broken, the crack of the both samples occurred at a section closer to the side that fabricated without Argon gas. This is because the presence of pores is gradually increase from section 2 to 3 due to the running out of Argon gas. The high presence of pores at the region causes high stress concentration that will affect the tensile results by concentrating the load into small area.

Finally, the hardness of three different section of the sample was evaluated using nanoindentation and microhardness test. Results show that; the hardness calculated at the section 3 is notably higher than other sections. The hardness for section 1 and 2 are almost similar. The high hardness in section 3 is due to the present of oxides in between the layers of the built object as observed by EDS analysis.

5.2 Future work

This work has investigated the effect of inert gas on the microstructure and mechanical properties of 316L stainless steel. Only two samples were used in this study. The effect of scanning speed was also investigated.

With regards to SLM processes, there are many directions that future research has the potential to go. With expanding on the research done here some areas to investigate in the future would be:

- Changing other machine parameters such as laser power to see how mechanical properties are affected.
- Testing other mechanical properties such as fatigue and compression strength.
- Testing other metallic materials such as 304 stainless steel to see how the microstructure and mechanical properties will be affected by the absence of the inert gas.

REFERENCES

Al-Meslemi, Y., Anwer, N., & Mathieu, L. (2018). Environmental Performance and Key Characteristics in Additive Manufacturing: A Literature Review. *Procedia CIRP, 69*, 148-153. doi:https://doi.org/10.1016/j.procir.2017.11.141

Baumann, F., & Roller, D. (2017). Additive Manufacturing, Cloud-Based 3D Printing and Associated Services—Overview. *Journal of Manufacturing and Materials Processing, 1*(2). doi:10.3390/jmmp1020015

Campbell, T. A., & Ivanova, O. S. (2013). 3D printing of multifunctional nanocomposites. *Nano Today, 8*(2), 119-120. doi:https://doi.org/10.1016/j.nantod.2012.12.002

Chang, F., Gu, D., Dai, D., & Yuan, P. (2015). Selective laser melting of in-situ Al4SiC4+SiC hybrid reinforced Al matrix composites: Influence of starting SiC particle size. *Surface and Coatings Technology, 272*, 15-24. doi:https://doi.org/10.1016/j.surfcoat.2015.04.029

Dadbakhsh, S., Hao, L., & Sewell, N. (2012). Effect of selective laser melting layout on the quality of stainless steel parts. *Rapid Prototyping Journal, 18*(3), 241-249. doi:10.1108/13552541211218216

DebRoy, T., Wei, H. L., Zuback, J. S., Mukherjee, T., Elmer, J. W., Milewski, J. O., . . . Zhang, W. (2018). Additive manufacturing of metallic components – Process, structure and properties. *Progress in Materials Science, 92*, 112-224. doi:https://doi.org/10.1016/j.pmatsci.2017.10.001

Demmer, A., Klingbeil, N., Klocke, F., Putz, M., Schmitt, R., & Vollmer, T. (2018). Target-oriented Analysis of Resource Consumption in Manufacturing Process Chains. *Procedia Manufacturing, 21*, 462-467. doi:https://doi.org/10.1016/j.promfg.2018.02.145

Faria, G. L. d., Godefroid, L. B., & Nery, F. V. (2016). Damage evolution in a tensile specimen of a ductile stainless steel. *Rem: Revista Escola de Minas, 69*(2), 175-183. doi:10.1590/0370-44672015690183

Fera, M., Fruggiero, F., Lambiase, A., Macchiaroli, R., & Pham, D. (2016). State of the art of additive manufacturing: Review for tolerances, mechanical resistance and production costs. *Cogent Engineering, 3*(1). doi:10.1080/23311916.2016.1261503

Ferrar, B., Mullen, L., Jones, E., Stamp, R., & Sutcliffe, C. J. (2012). Gas flow effects on selective laser melting (SLM) manufacturing performance. *Journal of Materials Processing Technology, 212*(2), 355-364. doi:10.1016/j.jmatprotec.2011.09.020

Gu, D., & Shen, Y. (2008). Processing conditions and microstructural features of porous 316L stainless steel components by DMLS. *Applied Surface Science, 255*(5), 1880-1887. doi:10.1016/j.apsusc.2008.06.118

Guan, K., Wang, Z., Gao, M., Li, X., & Zeng, X. (2013). Effects of processing parameters on tensile properties of selective laser melted 304 stainless steel. *Materials & Design, 50*, 581-586. doi:10.1016/j.matdes.2013.03.056

Herzog, D., Seyda, V., Wycisk, E., & Emmelmann, C. (2016). Additive manufacturing of metals. *Acta Materialia, 117*, 371-392. doi:https://doi.org/10.1016/j.actamat.2016.07.019

Kellens, K., Mertens, R., Paraskevas, D., Dewulf, W., & Duflou, J. R. (2017). Environmental Impact of Additive Manufacturing Processes: Does AM Contribute to a More Sustainable Way of Part Manufacturing? *Procedia CIRP, 61*, 582-587. doi:https://doi.org/10.1016/j.procir.2016.11.153

Kempen, K., Thijs, L., Humbeeck, J., & Kruth, J.-P. (2014). *Processing AlSilOMg by selective laser melting: Parameter optimisation and material characterisation*.

Kruth, J. P., Levy, G., Klocke, F., & Childs, T. H. C. (2007). Consolidation phenomena in laser and powder-bed based layered manufacturing. *CIRP Annals, 56*(2), 730-759. doi:https://doi.org/10.1016/j.cirp.2007.10.004

Lavernia, E. J., & Srivatsan, T. S. (2009). The rapid solidification processing of materials: science, principles, technology, advances, and applications. *Journal of Materials Science, 45*(2), 287-325. doi:10.1007/s10853-009-3995-5

Li R, L. J., Shi Y, Wang L, Jiang W. (2012). Balling behavior of stainless steel and nickel powder during selective laser melting process. *The International Journal of Advanced Manufacturing Technology, 59*, 10.

Liverani, E., Toschi, S., Ceschini, L., & Fortunato, A. (2017). Effect of selective laser melting (SLM) process parameters on microstructure and mechanical properties of 316L austenitic stainless steel. *Journal of Materials Processing Technology, 249*, 255-263. doi:10.1016/j.jmatprotec.2017.05.042

Maurice DR, C. T. (1990). The physics of mechanical alloying: a first report. Metallurgical Transactions A. *21:289-303.*

Olakanmi, E. O., Cochrane, R. F., & Dalgarno, K. W. (2015). A review on selective laser sintering/melting (SLS/SLM) of aluminium alloy powders: Processing, microstructure, and properties. *Progress in Materials Science, 74*, 401-477. doi:https://doi.org/10.1016/j.pmatsci.2015.03.002

Patterson, A. E., Messimer, S. L., & Farrington, P. A. (2017). Overhanging Features and the SLM/DMLS Residual Stresses Problem: Review and Future Research Need. *Technologies, 5*(2). doi:10.3390/technologies5020015

Paul, C. P., Ganesh, P., Mishra, S. K., Bhargava, P., Negi, J., & Nath, A. K. (2007). Investigating laser rapid manufacturing for Inconel-625 components. *Optics & Laser Technology, 39*(4), 800-805. doi:10.1016/j.optlastec.2006.01.008

Raghunath, N., & Pandey, P. M. (2007). Improving accuracy through shrinkage modelling by using Taguchi method in selective laser sintering. *International*

Journal of Machine Tools and Manufacture, 47(6), 985-995. doi:https://doi.org/10.1016/j.ijmachtools.2006.07.001

Rajabi, M., Vahidi, M., Simchi, A., & Davami, P. (2009). Effect of rapid solidification on the microstructure and mechanical properties of hot-pressed Al–20Si–5Fe alloys. *Materials Characterization, 60*(11), 1370-1381. doi:https://doi.org/10.1016/j.matchar.2009.06.014

Sames, W. J., List, F. A., Pannala, S., Dehoff, R. R., & Babu, S. S. (2016). The metallurgy and processing science of metal additive manufacturing. *International Materials Reviews, 61*(5), 315-360. doi:10.1080/09506608.2015.1116649

Sarkar, S., Siva Kumar, C., & Kumar Nath, A. (2017). Effect of mean stresses on mode of failures and fatigue life of selective laser melted stainless steel. *Materials Science and Engineering: A, 700*, 92-106. doi:https://doi.org/10.1016/j.msea.2017.05.118

Simchi, A., Petzoldt, F., & Pohl, H. (2003). On the development of direct metal laser sintering for rapid tooling. *Journal of Materials Processing Technology, 141*(3), 319-328. doi:https://doi.org/10.1016/S0924-0136(03)00283-8

Tan, J. H., Wong, W. L. E., & Dalgarno, K. W. (2017). An overview of powder granulometry on feedstock and part performance in the selective laser melting process. *Additive Manufacturing, 18*, 228-255. doi:https://doi.org/10.1016/j.addma.2017.10.011

Yang, S., & Evans, J. R. G. (2004). A multi-component powder dispensing system for three dimensional functional gradients. *Materials Science and Engineering: A, 379*(1), 351-359. doi:https://doi.org/10.1016/j.msea.2004.03.047

Yasa, E., & Kruth, J. P. (2011). Microstructural investigation of Selective Laser Melting 316L stainless steel parts exposed to laser re-melting. *Procedia Engineering, 19*, 389-395. doi:10.1016/j.proeng.2011.11.130

Zhang, B., Dembinski, L., & Coddet, C. (2013). The study of the laser parameters and environment variables effect on mechanical properties of high compact parts elaborated by selective laser melting 316L powder. *Materials Science and Engineering: A, 584*, 21-31. doi:https://doi.org/10.1016/j.msea.2013.06.055